Spring 5-4-2024

Individual Differences in Age and Testosterone are Uniquely Associated with Neural Oscillatory Activity Serving Verbal Working Memory in Children and Adolescents

Abraham D. Killanin
University of Nebraska Medical Center

INDIVIDUAL DIFFERENCES IN AGE AND TESTOSTERONE ARE UNIQUELY ASSOCIATED WITH NEURAL OSCILLATORY ACTIVITY SERVING VERBAL WORKING MEMORY IN CHILDREN AND ADOLESCENTS

By

Abraham D. Killanin

A DISSERTATION

Presented to the Faculty of the Graduate College at the University of Nebraska

In Partial Fulfillment of Requirements

For the Degree of Doctor of Philosophy

Interdisciplinary Graduate Program in Biomedical Sciences

(Neuroscience)

Under the Supervision of Drs. Tony Wilson and Soonjo Hwang

University of Nebraska Medical Center

Omaha, Nebraska

February, 2024

Supervisory Committee:

Elizabeth Heinrichs-Graham, Ph.D.

Jennifer Blackford, Ph.D.

Daniel Gih, M.D.

ACKNOWLEDGEMENTS

Principally, I am indebted to my mentor, Dr. Tony Wilson, who has patiently led me since 2017 with a belief in my ability far exceeding my own most times. He has taught me to approach hypotheses and analytic strategy with informed inquiry and has instilled in me a spirit of excellence and discipline that I will take into the rest of my career. Amidst his many roles as a director, teacher, mentor, husband, father, and son, he has stood as a steadfast pillar in this oftentimes rocky terrain of graduate training.

I humbly thank my mother and father, whose wildest, unimaginable dreams I am currently living. I would not be the man or the student that I am today without their “steady rod and gentle hands.” The path I have taken to reach this doctoral degree is marked by many unseen and unheard ways that they have adjusted their lives to provide opportunities for me. For that, my heart overflows with gratitude.

Much of my work would not be possible without my colleagues, past and present, in the DICoN Lab and the Institute for Human Neuroscience, including Elizabeth Heinrichs-Graham, Christine Embury, Alex Wiesman, Rachel Spooner, Yasra Arif, Mikki Schantell, Seth Springer, Chloe Meehan, Thomas Ward, Jake Son, Maggie Rempe, Kellen McDonald, Morgan Busboom, Nathan Petro, Giorgia Picci, Brittany Taylor, Max Kurz, Nichole Knott, Rebecca Losh, Melissa Welch, Lisa Houseman, Hannah Okelberry, and Grant Garrison.

This research was financially supported by grants to my advisor, Dr. Tony Wilson, from the National Institutes of Health (R01-MH1121101, P20-GM144641). Additionally, my training was supported by a Ruth L. Kirschstein Predoctoral Fellowship from the National Institute on Mental Health (F30-MH130150). Finally, I thank the participants who made our research possible.

ABSTRACT

During the sensitive period of adolescence, the human brain undergoes dynamic changes in structure and function resulting in vast executive function gains. Verbal working memory (VWM) is one executive function that serves as a foundation to language acquisition, reading, and learning. Many have examined the development of VWM in youth, but few have probed age-related changes in the underlying neural oscillatory dynamics, and none have examined testosterone-related changes. We recorded magnetoencephalography during a modified Sternberg VWM task in 82 youth participants aged 6 – 14 years old and collected salivary testosterone samples. Significant oscillatory responses were identified and imaged using a beamforming approach and the resulting whole-brain maps were probed for developmental effects during the encoding and maintenance phases. First, we identified cortical regions in which oscillatory power significantly covaried with chronological age (Chapter 1), and then we quantified the functional connectivity between these regions, using phase-locking value, as a function of chronological age (Chapter 2). Lastly, we probed whole-brain maps for cortical regions exhibiting significant relationships between oscillatory power and endogenous testosterone hormone levels, controlling for age (Chapter 3). These results extend the existing literature on working memory development by showing strong associations between oscillatory dynamics and unique development measures across a distributed network.

TABLE OF CONTENTS

LIST OF FIGURES

LIST OF ABBREVIATIONS

DICS	Dynamic Imaging of Coherent Sources
DHEA	Dehydroepiandrosterone
DHEA-S	Dehydroepiandrosterone sulfate
dlPFC	Dorsolateral prefrontal cortex
EEG	Electroencephalography
fMRI	Functional magnetic resonance imaging
MEG	Magnetoencephalography
OTC	Occipito-temporal cortex
PFC	Prefrontal cortex
PLV	Phase-locking value
TPJ	Temporal-parietal junction
VWM	Verbal Working Memory
WM	Working Memory

INTRODUCTION

Measures of Cortical Development During Adolescence

As children mature into adolescence, they develop a greater ability to hold information in mind and strategically control or coordinate thoughts with behaviors (*1*). Studies have shown that as age increases the neural cortex is dynamically re-structured, with grey matter loss beginning in lower-order sensorimotor regions and moving to higher-order association cortices (*2*). Myelination increases, improving the speed of information transfer, and experience-dependent synaptic pruning occurs to remove infrequently used neural connections. A large body of work has related this cortical maturation to the improvements in executive functions during this developmental stage, and it ultimately points to adolescence as a sensitive period for the development of higher-order cognitive functions (*3, 4*).

Although chronological age is the main variable with which neurocognitive development is often measured, there are other biological factors that also affect maturational processes. During adolescence, pubertal hormones drastically increase to effect changes in the brain and body. The two stages of puberty, as defined by adrenal and gonadal hormone production, are adrenarche and gonadarche. Adrenarche can start as early as 6 and is marked by the adrenal glands producing large amounts of dehydroepiandrosterone (DHEA) and its sulfate DHEA-S. DHEA has been shown to stimulate neurogenesis and affect pre- and post-synaptic binding sites through its conversion to testosterone, estrogen, and di-hydrotestosterone (*5*). These actions suggest that adrenarche extends brain development and synaptogenesis to facilitate adolescent social learning. The second stage of puberty, gonadarche, begins around 10 – 11 years old. It is triggered by the release of gonadotropin-releasing hormone from the hypothalamus, signaling the gonads to increase testosterone and estradiol production,

resulting in the development of secondary sex characteristics and menarche in females (*6*).

Studies examining the effects of testosterone on cortical structural development vary between sex, morphological measurement of interest (e.g., surface area or cortical thickness), and brain region. Differences are due to whether age is a variable that is controlled for, whether samples include one or both sexes, and the time point at which hormones are measured. For example, associations have been reported between higher testosterone and smaller relative grey matter volumes (*7*), but larger global grey matter volumes when age is controlled for (*8*). Yet another study reported higher testosterone correlated with smaller total gray matter volumes in 10-13-year-old girls but not boys 11-14 (*9*). Despite the differences in findings within human studies, animal studies offer a unique understanding of testosterone's effect on neural morphology, with evidence showing that testosterone's effects are exerted mainly through androgen receptors. For the most part, studies utilizing gonadectomized mice have shown that the absence of testosterone is associated with aberrant pyramidal dendrite morphology (*10, 11*). Generally, evidence suggests that early in puberty, testosterone levels are associated with a great deal of structural change (*12*).

Working Memory and Neural Substrates in Adolescence

Working memory (WM), or the short-term retention of information in mind for an eventual goal, is an executive function that forms the foundation of most human learning and decision-making (*13*). It emerges during early childhood and continues to develop as the neocortex changes, with maturational improvements observed well into young adulthood (*14, 15*). Studies have demonstrated its strong association with mathematic and reading abilities (*13, 16, 17*), and due to its ubiquitous nature in cognitive processing, it is also a shared deficit in psychiatric disorders (*18, 19*).

The initial phase of WM is encoding when the stimulus that needs to be remembered is initially perceived. Once a stimulus has been encoded, it is held in memory until it is eventually retrieved. While in memory stores, however, it is subject to forgetting or interference from other internal representations of non-relevant stimuli. In this case rehearsal processes are required to refresh information and keep it from decay. One of the most influential cognitive models of working memory is the multi-component model proposed by Baddeley and Hitch (*20*). Baddeley's model proposes that a central executive governs the transfer of information into and out of memory stores and directs attention to relevant stimuli. Serving the central executive are sub-systems that respond to stimulus properties; the phonological loop governs verbal stimuli while the visuospatial sketchpad entails visual or spatial information. In children and adolescents, these components are in place by age 7, and with development, the relationships between the central executive and the two sub-components are fortified (*21*).

Studies using functional magnetic resonance imaging (fMRI) found that protracted maturation of the neocortex leads to functional differences in working memory between children and adolescents. Generally, with increasing age there is greater recruitment of left frontal cortices, left precuneus, and left inferior parietal cortices, and decreased recruitment of right superior frontal, left postcentral, and left limbic cingulate gyrus (*22*). Researchers believe this reflects increased recruitment of core regions in the working memory network and the release of immature regions that are no longer needed. While there is a growing interest in the effects of puberty on executive functions, there are few investigations relating endogenous levels of pubertal hormones, like testosterone, to the neural underpinnings of working memory processing.

Many studies using fMRI have probed the effects of age in key developing cortical regions on verbal working memory (VWM) processes, using the N-back and delayed-match-to-sample tasks (*23-25*). These investigations have been critical to bridging the gap

between structure and function. However, the blood oxygen level-dependent response utilized in fMRI studies lack the temporal precision to reliably disentangle neural processes during the different phases of VWM. It is also difficult to resolve these components using an N-back task, as they require simultaneous encoding, maintenance, and rehearsal, often in various orders. The Sternberg item-recognition task, one of many delayed-match-to-sample tasks, successfully divides working memory into subcomponent processes such that participants sequentially complete encoding and maintenance. Use of this task provides a characteristic understanding of the information flow from initial stimulus perception to maintenance rehearsal.

An Oscillatory Perspective of Working Memory

Assemblies of neurons exhibit periodic fluctuations in excitability that can modulate information transmission and dynamically respond to task demands via synchronization between different cortical regions (*26*). Neuronal oscillations support cognitive processing, and through their study provide a link between single-neuron activity and behavior (*27*). Electroencephalography (EEG) and magnetoencephalography (MEG) have been utilized to capture the temporal dynamics of oscillatory activity at the millisecond level, using the electrical and magnetic fields emanating from the scalp, respectively. However, MEG offers a superior analytic prospect, as signal distortion is far reduced. With sufficient spatial resolution, MEG data offers a look into neural network activity at a temporal resolution that is behaviorally relevant. Further, MEG directly measures neuronal activity and functional connectivity, without the intervening effects of neurovascular processes.

By studying the oscillatory underpinnings of working memory, researchers have gained insight into the spectral components of network-level communication during encoding and maintenance. Theta (4 – 7 Hz) activity in frontal cortices and alpha (8 – 14 Hz) activity have been shown to increase as a function of memory load during maintenance or task difficulty (*28-30*). During encoding, studies found that alpha-beta (9

– 16 Hz) desynchronous activity in left dorsolateral prefrontal cortex and superior temporal cortices becomes stronger during encoding as a function of time. This activity is sustained throughout much of maintenance. In visual cortices during encoding, desynchronous activity becomes weaker with time, and evolves into strong synchronizations during maintenance (*31*). While few studies have examined the development of the spectro-temporal oscillatory dynamics serving working memory, results suggest that developmentally sensitive regions may mature at different times between males and females, depending on the age range studied. Patterns of developmental change may also be spectrally and temporally specific, with unique effects found in different cortical regions during encoding and maintenance (*32-34*).

Goals of the Current Study

The studies herein aim to delineate the pattern of developmental change in the neural oscillatory underpinnings of VWM. Using chronological age (Chapter 1) and endogenous testosterone levels (Chapter 3), measured by salivary hormone analysis, these studies will distinguish the cortical regions that exhibit the greatest change in population-level oscillatory activity among typically-developing youth between the ages of 6 and 14. The functional communication between these developmentally sensitive regions will also be characterized (Chapter 2) to provide context for how patterns of developmental change contribute to verbal working memory processing. Quantifying the relationships between oscillatory activity and markers of development, these studies will provide a strong foundation for future studies in typically developing youth and youth with psychopathological disorders, further advancing the study of neurodevelopment.

CHAPTER 1: CHRONOLOGICAL AGE AND OSCILLATORY POWER SERVING VERBAL WORKING MEMORY IN CHILDREN AND ADOLESCENTS

The material presented in this chapter currently under review as Killanin, Ward, Embury, Calhoun, Wang, Stephen, Picci, Heinrichs-Graham, and Wilson, 2024, Better with Age: Developmental Changes in Oscillatory Activity During Verbal Working Memory Encoding and Maintenance

Introduction:

Working memory improves from childhood to adolescence as youth become more skilled at briefly holding and manipulating information for better learning and planning (*17*). These behavioral improvements are thought to reflect increasing functional specialization of brain regions supporting stimulus encoding and maintenance during working memory, with mature levels of processing requiring efficient functional integration of information across these neural regions (*35*). Such developmental changes in the prefrontal cortex have been widely reported (*1, 23, 36, 37*), and this region's involvement in working memory processing has been suggested to aid in information transfer across multiple cortical regions, especially in cases where more than one cognitive operation is required (*38*). As part of the fronto-parietal network, the left inferior parietal cortex also undergoes structural and functional changes with age and has been associated with processes such as phonological encoding (*22, 39-41*).

While our understanding of the key brain regions involved in working memory processing has grown considerably, the inherent dynamics within these neural regions are not fully understood. Neural processing during discreet stages of working memory can be studied using the Sternberg task, which requires individuals to encode stimuli into memory stores and briefly maintain these representations for eventual retrieval and differs from the N-back task which elicits parallel encoding and maintenance operations (*42*). Numerous magnetoencephalography (MEG) studies have reported stronger alpha oscillations (8-12

Hz; decreases in power) during encoding in bilateral occipital cortices, which tend to gradually move anteriorly during maintenance into left-lateralized language regions, like the left temporal, supramarginal, and prefrontal cortices (*31, 32, 43-46*). Concurrently, during maintenance, the initial alpha response in bilateral occipital cortices progressively weakens and becomes an increase in alpha power within parieto-occipital regions (*31, 45, 47*). In addition, multiple studies have reported increased frontal theta during maintenance that scales with task difficulty, suggesting a possible role in attention and/or executive function (*28, 48-50*).

To characterize developmental changes in the oscillatory dynamics serving working memory, one study used a six-load version of the Sternberg task in a sample of typically developing 9-to-14-year-olds (*32*). Aside from the improvements in performance expected with increased age, this study did not find significant main effects of age (i.e., across both sexes). Instead, they found age-by-sex interactions with older females exhibiting significantly stronger alpha oscillations during encoding in the right inferior frontal cortex than younger females, while older males showed stronger increases in alpha during maintenance compared to younger males in right occipital, right cerebellar, and parietal cortices. Embury et al. suggested that the prefrontal and posterior cortices that support top-down executive control and storage during working memory have developmental trajectories that briefly diverge in a sex-specific manner before converging later in young adulthood (*32*).

Although MEG working memory studies have been conducted in child and adolescent samples (*32-34, 51*), only one has probed age-related changes in a typically developing sample (*32*). In the current investigation, we examined a younger (6-14 years-old), and larger, sample of typically developing youths and focused on the neural oscillatory activity that supports the encoding and maintenance phases of VWM. By examining a younger sample than previous studies, we hoped to capture unique

developmental patterns that emerge as networks become more refined during adolescence. For example, as children learn to read, verbal rehearsal becomes more reliable, enabling them to recode visual stimuli more readily into their phonological forms for maintenance (*21*). We hypothesized that alpha oscillatory activity would become stronger in older participants, during both encoding and maintenance periods, in left-lateralized language regions. We also hypothesized that we would identify significant sex differences in these patterns of developmental change in the neural oscillatory dynamics serving working memory.

Methods:

Participants

A total of 106 participants between the ages of 6 and 14 years old (*M*=10.07 years, *SD* = 2.53; 50 females; 11 left-handed) were recruited from the community, as part of the Developmental Multimodal Imaging of Neurocognitive Dynamics study, an NIH supported project employing an accelerated longitudinal design to investigate brain and cognitive development (R01-MH121101). Of note, due to the accelerated longitudinal design of the study, 10-year-olds were not enrolled. The current investigation utilizes cross-sectional data collected exclusively during year one of the study. Participants were all typically developing primary English speakers and did not have diagnosed psychiatric or neurological conditions, previous head trauma, learning disability, or non-removable ferromagnetic material (e.g., orthodonture). After a complete description of the study, written informed assent and consent was obtained from the child and child's parent or legal guardian, respectively. All procedures were completed at the University of Nebraska Medical Center and approved by the University of Nebraska Medical Center Institutional Review Board.

Experimental Paradigm

Participants completed a modified Sternberg VWM task similar to those used in several previous studies of adults (*31, 43, 46, 52, 53*) and youths (*32*). Participants rested their right hand on a custom five-finger button response pad directly connected to the MEG system so that each button press sent a TTL pulse to the acquisition computer in real-time, enabling behavioral responses to be temporally synced with the MEG data. Accuracy and reaction time were calculated offline. Participants were shown a centrally presented fixation cross embedded in a 5x5 grid for 1,000 ms (i.e., baseline period). An array of four consonants then appeared at fixed locations within the grid for 2,000 ms (i.e., encoding period). The letters disappeared from the array leaving an empty grid shown for 2,000 ms (i.e., maintenance period), during which participants had to maintain the encoded letters from the previous phase. A probe letter then appeared on the grid for 1,500 ms (i.e., retrieval period), and participants were instructed to respond with their right index if the probe letter was found in the previous array of letters or with their middle finger if it was not. Participants completed 128 trials, split equally and pseudorandomized between in- and out-of-set trials, for a total run time of about 15 minutes (see Figure 1). Visual stimuli were presented using the E-Prime 2.0 software (Psychology Software Tools, Pittsburgh, PA), and back-projected onto a semi-translucent nonmagnetic screen at an approximate distance of 1.07 m, using a Panasonic PT-D7700U-K model DLP projector with a refresh rate of 60 Hz and a contrast ratio of 4000:1.

MEG Data Acquisition

Participants sat in a nonmagnetic chair within a one-layer magnetically shielded room with active shielding engaged during MEG recording. Neuromagnetic responses were sampled continuously at 1 kHz with an acquisition bandwidth of 0.1 – 330 Hz using an MEG system with 306 magnetic sensors (MEGIN, Helsinki, Finland). MEG data from each subject were individually corrected for head motion (MaxFilter v2.2; MEGIN) and

subjected to noise reduction using the signal space separation method with a temporal extension (*54, 55*).

Structural MRI Data Acquisition and MEG Co-registration

A 3T Siemens Prisma scanner equipped with a 32-channel head coil was used to collect high-resolution structural T1-weighted MRI data from each participant (TR: 24.0 ms; TE: 1.96 ms: field of view: 256 mm; slice thickness: 1 mm with no gap; in-plane resolution: 1.0 x 1.0 mm). Structural volumes were aligned parallel to the anterior and posterior commissures and transformed into standardized space. Each participant's MEG data were co-registered with their MRI data using BESA MRI (Version 2.0). After source imaging (beamformer), each subject's functional images were also transformed into standardized space using the transform previously applied to the structural MRI volume, and spatially resampled.

MEG Time-Frequency Decomposition and Statistical Analysis

For a more detailed description of our methodological approach, see Wiesman and Wilson (*56*). Cardiac and ocular artifacts were visually inspected and removed from the data using signal-space projection, which was accounted for during source reconstruction (*57*). The continuous magnetic time series was divided into 5,900 ms epochs, with stimulus presentation (i.e., 5x5 grid containing four consonants) defined as 0 ms and the baseline defined as the -400 to 0 ms time window (i.e., fixation period; Figure 1). Only correct trials were used for analysis. Epochs containing artifacts were rejected based on a fixed threshold method, which was supplemented with visual inspection. Briefly, the distributions of amplitude and gradient values per participant were computed using all correct trials, and the highest amplitude/gradient trials relative to the total distribution were excluded. Notably, individual thresholds were set for each participant for both amplitude (M = 2145.88 fT/cm, SD = 909.0) and gradient (M = 539.34 fT/(cm*ms), SD = 258.4) due to

differences among individuals in head size and sensor proximity, which strongly affect MEG signal amplitude. Note that an average of 87.20 (SD: 12.1) trials per participant remained for further analysis and the number of accepted trials was not significantly correlated with age and did not differ between sexes (see Results).

Artifact-free epochs were then transformed into the time-frequency domain using complex demodulation with a resolution of 1.0 Hz and 50 ms (*58, 59*). The resulting spectral power estimations per sensor were averaged over trials to generate time-frequency plots of mean spectral density. These sensor-level data were then normalized per frequency bin using the mean power during the –400 to 0 ms baseline period. The specific time-frequency windows used for imaging were determined by statistical analysis of the sensor-level spectrograms across the entire array of gradiometers. Each data point in the spectrogram was initially evaluated using a mass univariate approach based on the general linear model. To reduce the risk of false-positive results while maintaining reasonable sensitivity, a two-stage procedure was followed to control for Type 1 error. In the first stage, paired-sample t-tests against baseline were conducted on each data point and the output spectrogram of t-values was threshold at $p < .05$ to define time-frequency bins containing potentially significant oscillatory deviations across all participants. In stage two, time-frequency bins that survived the threshold were clustered with temporally and/or spectrally neighboring bins that were also below the ($p < .05$) threshold, and a cluster value was derived by totaling all t-values of all data points in the cluster. Nonparametric permutation testing was then used to derive a distribution of cluster-values, and the significance level of the observed clusters (from stage one) was tested directly using this distribution (*60, 61*). For each comparison, 10,000 permutations were computed to build a distribution of cluster values. Based on these analyses, time-frequency windows that

contained a significant oscillatory event relative to the permutation testing null were subjected to the beamforming analysis.

MEG Source Imaging and Statistics

Cortical oscillatory activity was imaged through an extension of the linearly constrained minimum variance vector beamformer (*62, 63*) using the Brain Electrical Source Analysis (BESA 7.0) software. This approach, commonly referred to as dynamic imaging of coherent sources (DICS), applies spatial filters to time-frequency sensor data to calculate voxel-wise source power for the entire brain volume. The single images are derived from the cross-spectral densities of all combinations of MEG gradiometers averaged over the time-frequency range of interest, and the solution of the forward problem for each location on a 4.0 × 4.0 × 4.0 mm grid specified by input voxel space. Following convention, we computed noise-normalized, source power per voxel in each participant using active (i.e., task) and passive (i.e., baseline) periods of equal duration and bandwidth. Such images are typically referred to as pseudo-*t* maps, with units (pseudo-*t*) that reflect noise-normalized power differences (i.e., active vs. passive) per voxel. This generated participant-level pseudo-*t* maps for each time-frequency-specific response identified in the sensor-level permutation analysis, which was then transformed into standardized space using the transform previously applied to the structural MRI volume and spatially resampled.

Resultant pseudo-*t* maps were averaged within participants across the time windows used to image neural activity during encoding and maintenance periods, separately. The averaged source maps did not include segments representative of time windows spanning two different phases of the task (e.g., encoding and maintenance). Developmental associations with neural activity were examined via whole-brain voxel-wise correlations with chronological age across the entire sample. Whole-brain correlation

maps were then computed separately for males and females, followed by whole-brain bivariate correlation coefficient comparisons computed via Fisher's Z-transformation. Resultant voxel-wise maps of z-scores represented the normalized difference between males and females in the development-by-oscillatory power (pseudo-t units) relationship. To account for multiple comparisons, a significance threshold of $p < .005$ was used in all statistical maps to identify significant clusters, in addition to a cluster threshold of 8 contiguous voxels.

Results:

Demographic and Behavioral Results

Of the 106 participants who completed the modified Sternberg VWM task, we excluded 15 for poor accuracy (<60% total trials completed correctly) and 9 for MEG artifacts. Therefore, the final sample analyzed consisted of 82 participants (M = 10.38 years, SD = 2.50; 38 females; 9 left-handed), and age did not significantly differ by sex ($t(80) = -.77$, $p = .44$). To ensure that the MEG data of the final sample was not biased by age, we tested for a relationship between age and the number of trials retained for analysis. The number of trials retained was not significantly correlated with age ($r = .15$, $p = .17$) and did not significantly differ by sex ($t(80) = .69$, $p = .49$). Average accuracy on the VWM task was 84.10% (SD = 10.24) and average reaction time was 1191.08 ms (SD = 248.15). Accuracy was significantly positively correlated with age such that older participants performed significantly better than younger participants on the task ($r = .59$, $p < .001$). Reaction time was significantly negatively correlated with age such that older participants responded significantly faster than younger participants ($r = -.65$, $p < .001$; Figure 1). An independent samples t-test showed that males and females did not significantly differ in accuracy ($t(80) = 0.29$, $p = .77$) or reaction time ($t(80) = 1.48$, $p = .14$).

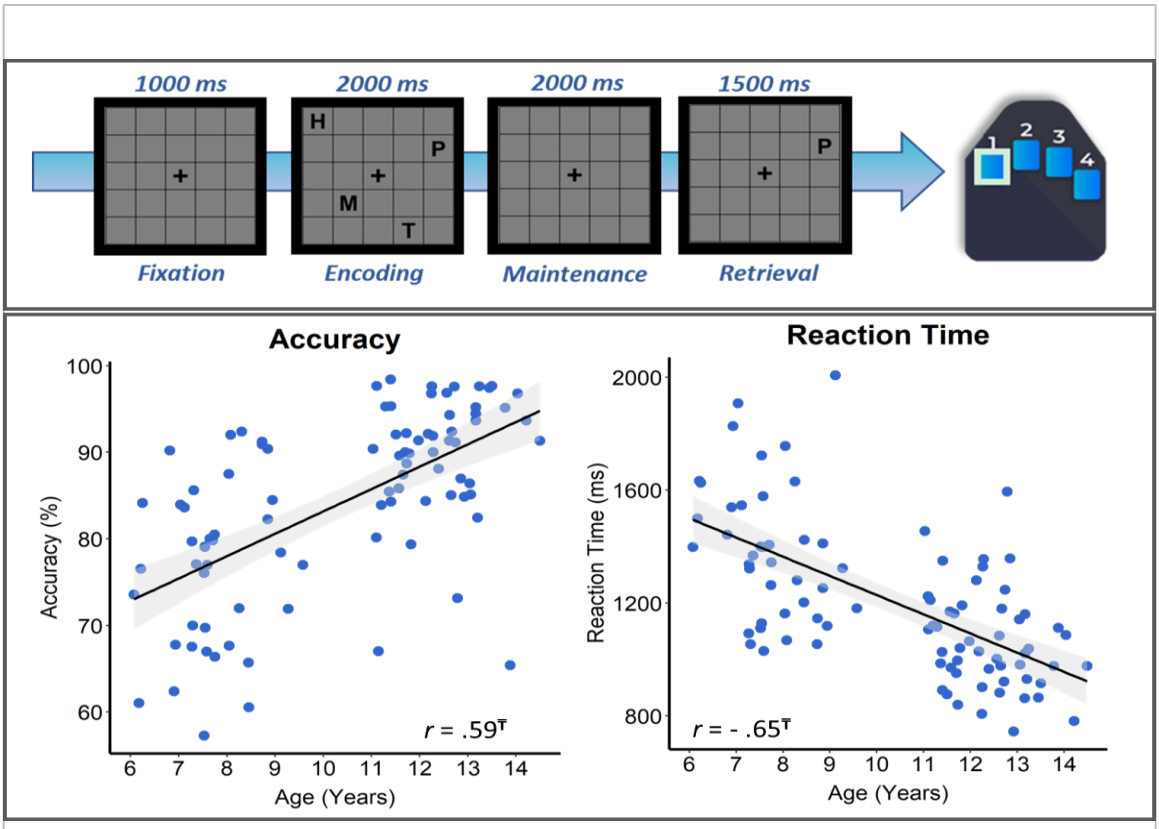

Figure 1: Modified sternberg VWM task and behavior.
(Top) Example trial of the modified Sternberg working memory task along with the corresponding correct response. (Bottom) Accuracy and reaction time were significantly correlated with chronological age.
Ŧ $p < .001$.

MEG Sensor-Level and Source-Level Results

Statistical examination of sensor-level time-frequency spectrograms showed two responses during the encoding period. A significant increase in theta (4-7 Hz) power relative to baseline began 100 ms after encoding onset and extended until about 500 ms, before gradually dissipating until 2200 ms. A significant decrease in alpha (8-12 Hz) began 400 ms after encoding onset and extended until 2000 ms. During the maintenance period there was a strong increase in alpha (9-14 Hz), which began 550 ms after the encoding grid off-set. This lasted for approximately 350 ms before dissipating into more narrow alpha activity (8-12 Hz), which lasted until near the end of the maintenance period (Figure 2; $p < 0.0001$, permutation corrected). These alpha and theta responses were divided into

400 ms non-overlapping time bins, with source reconstruction performed on the resultant time-frequency windows of interest. Specifically, we applied a beamformer to the following windows: 4-7 Hz from 100 to 500 ms, 8-12 Hz from 400 to 2000 ms, 9-14 Hz from 2550-2900 ms, and 8-12 Hz from 3100-3900 ms.

Average beamformer images across all participants revealed that the early theta response was strongest in bilateral occipital cortices, while the alpha response during encoding began in bilateral occipital regions and extended anteriorly to include left temporal regions as encoding progressed. During maintenance, increases in alpha (9-14 Hz) were primarily seen in right parieto-occipital cortices.

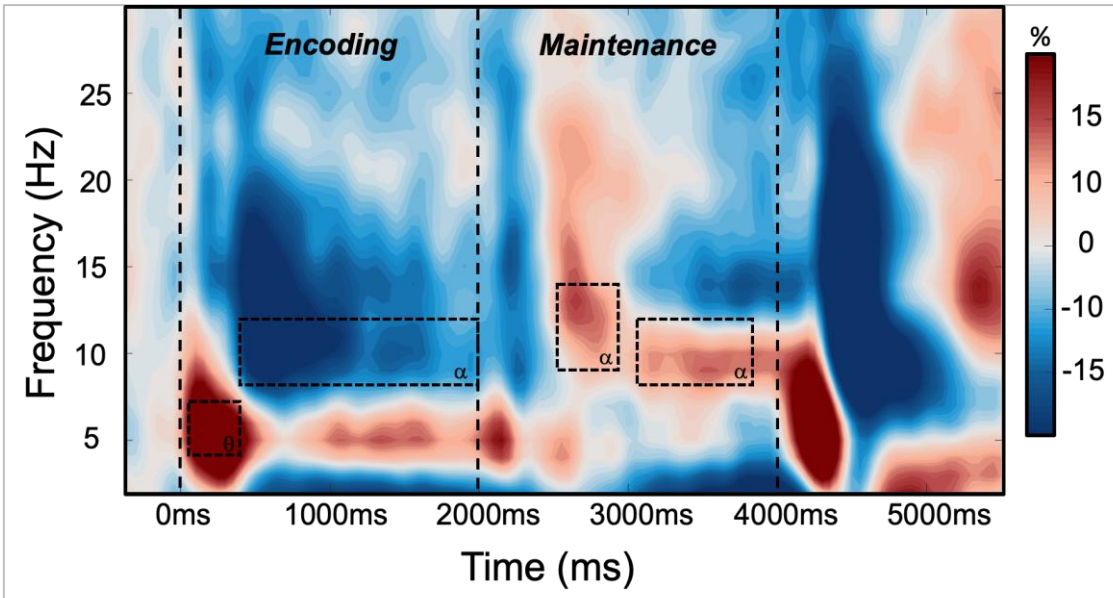

Figure 2: Grand-averaged MEG sensor-level spectrogram.

Grand-averaged time-frequency spectrogram taken from a representative sensor (MEG2043). Time is denoted on the x-axis (0.0 s = encoding onset) and frequency (Hz) is shown on the y-axis. The time-frequency windows used for subsequent beamforming are denoted by the dashed black boxes. The spectrogram is shown in percent power change from baseline, with the color scale shown to the right of the spectrogram.

Developmental Changes in Neural Oscillatory Responses

Whole-brain, voxel-wise correlations indicated that theta responses during encoding were positively correlated with age in left (r = .33, $p < .005$; Figure 3A) and right

(*r* = .40, *p* < .001; Figure 3B) occipital cortices, indicating that older youth had stronger theta responses than their younger peers. Additionally, during encoding, alpha (8-12 Hz) oscillations became stronger (i.e., more negative) with increasing age in left dorsal prefrontal (*r* = -.36, *p* < .001; Figure 3C), supramarginal (*r* = -.55, *p* < .001; Figure 3E), and occipito-temporal cortices (OTC; *r* = -.34, *p* < .005; Figure 3E). Conversely, alpha oscillations during encoding became weaker with increasing age in the anterior right

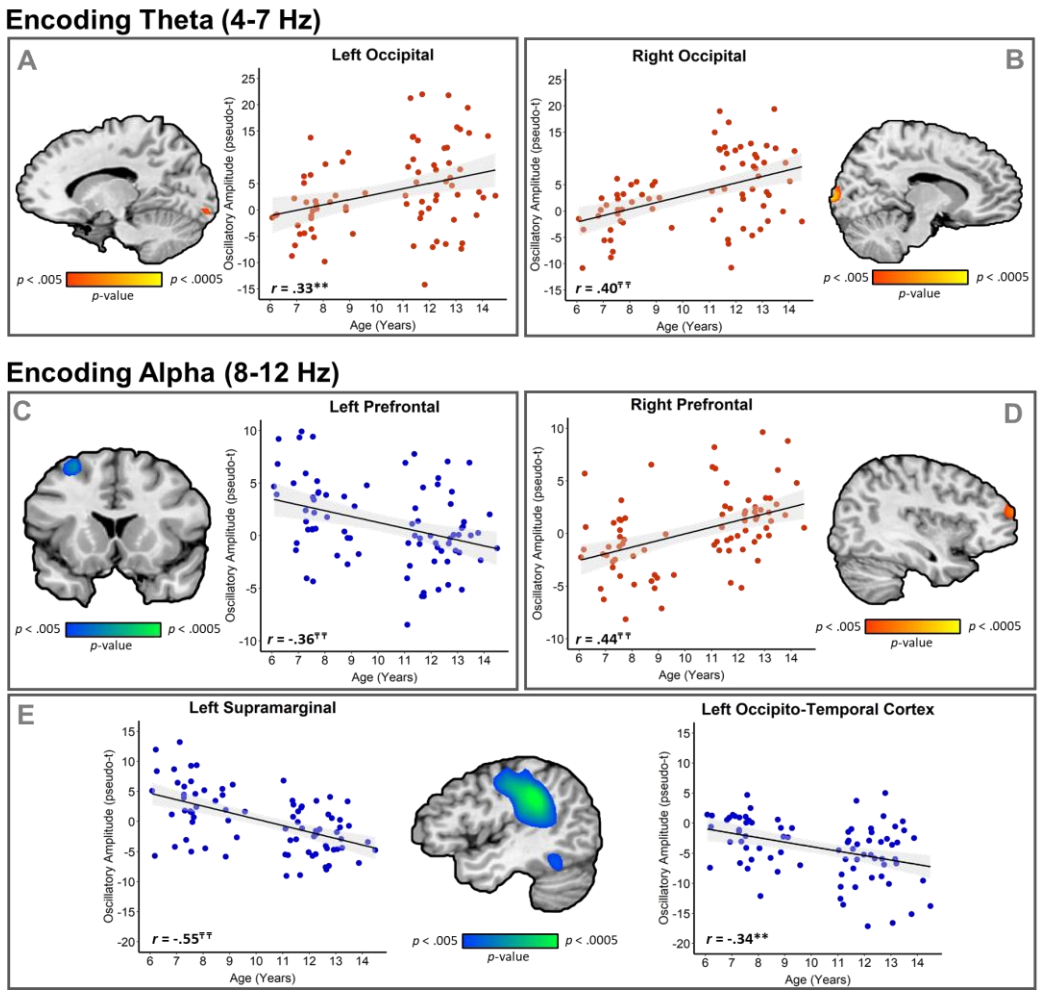

Figure 3: Developmental alterations in the neural oscillations serving working memory encoding.

Whole-brain correlation maps and associated scatterplots showing the relationship at the peak voxel, with age in years on the x-axes and oscillatory amplitude in pseudo-t units on the y-axes. (A-B) Theta oscillations became stronger with increasing age in the bilateral occipital cortices. (C-E) Alpha oscillations became stronger with increasing age in the left dorsal prefrontal cortices, left supramarginal, and left occipito-temporal cortices, while the opposite pattern was observed in the right anterior prefrontal cortices. **$p < .005$; ŦŦ$p < .001$.

prefrontal cortex (r = .44, p < .001; Figure 3D). During maintenance (3100 – 3900 ms), alpha oscillations became stronger with increasing age within the right occipital cortices (r = -.36, p < .005; Figure 4A), right parietal cortices (r = -.37, p < .001; Figure 4B), left prefrontal cortices (r = -.38, p < .005; Figure 4C), and left OTC (r = -.38, p < .001; Figure 4C). Finally, a significant effect of age was also found in the motor cortex, however because this study focused on working memory processing, we did not probe this finding further.

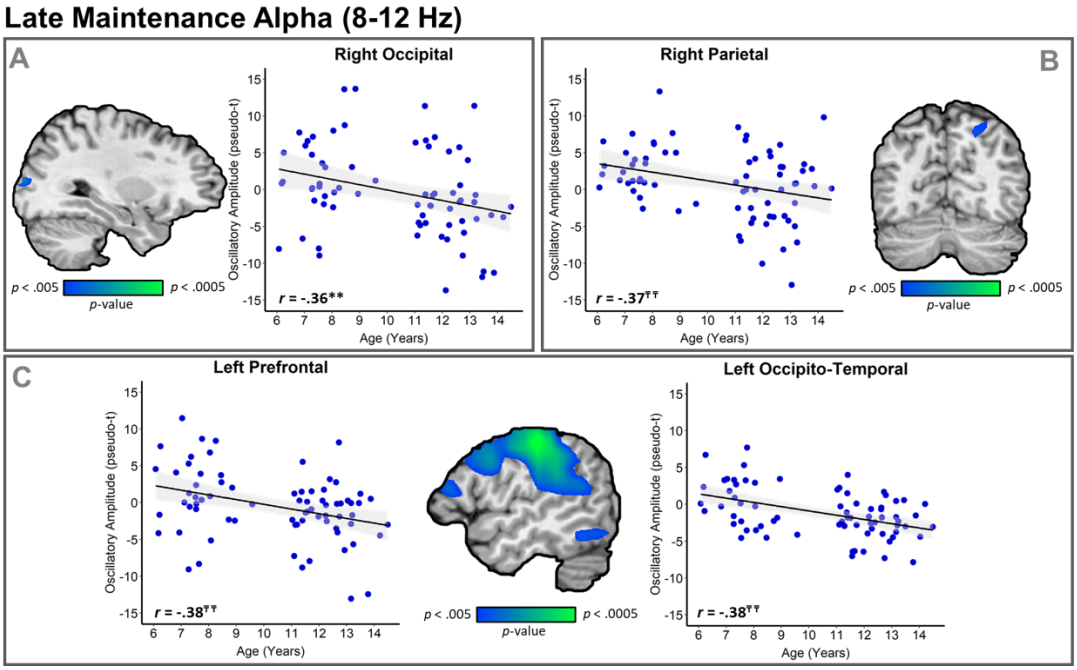

Figure 4: Developmental alterations in the neural oscillations serving working memory Maintenance.

Whole-brain correlation maps and associated scatterplots showing the relationship at the peak voxel, with age in years on the x-axes and oscillatory amplitude in pseudo-t units on the y-axes. (A-C) Alpha oscillations became stronger with increasing age in the right occipital cortices, right parietal, left prefrontal, and left occipito-temporal cortices.
**p < .005; ŦŦp < .001.

Sexually-divergent Developmental Changes in Oscillatory Strength

Age-by-sex interaction effects on theta power during encoding were found in two distinct regions of the right cerebellum. More posteriorly, theta oscillations became weaker

with increasing age in females, whereas males exhibited the inverse pattern (Z = 3.15, p < .005; Figure 5A). Anterior to this effect, there was a patch of right cerebellar cortices where theta power became weaker with increasing age in males, with the opposite pattern in females (Z = 3.06, p < .005; Figure 5B). In addition, age-by-sex interactions were detected in the right superior temporal gyrus during the early maintenance phase, with females exhibiting stronger alpha oscillations with increasing age and males showing the reverse pattern (Z = -3.62, p < .005; Figure 5C). Further, the same pattern of interactions were also detected in left cerebellar (Z = -3.36, p < .001) and left occipital cortices (Z = -2.91, p < .005).

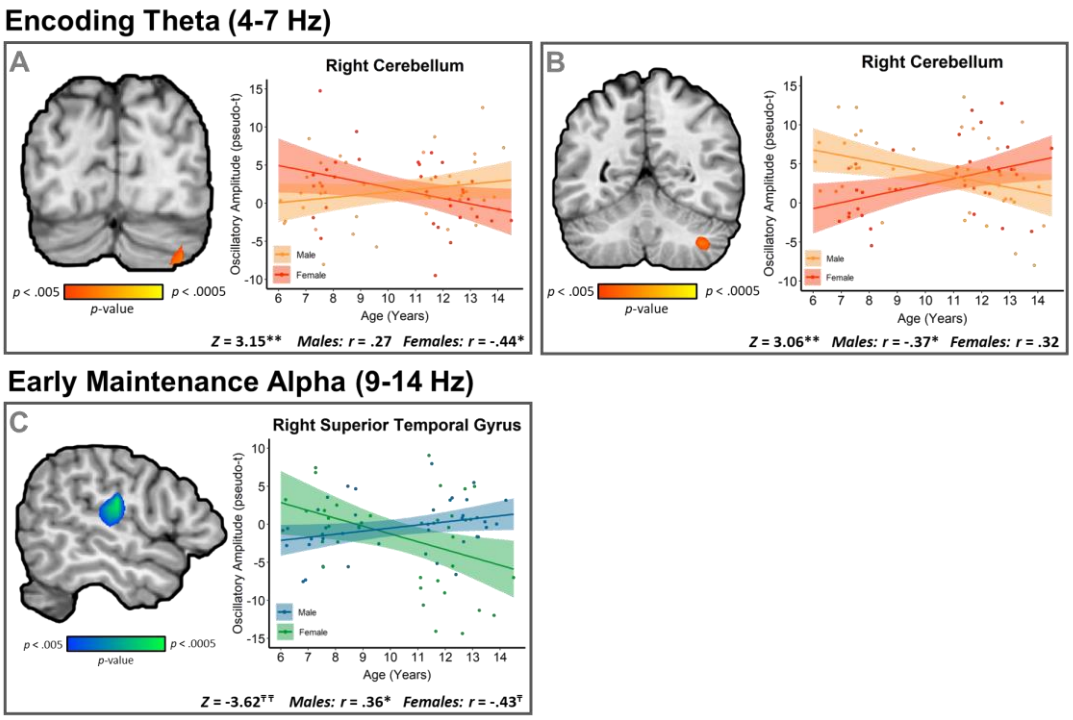

Figure 5: Sexually divergent developmental patterns of neural oscillations serving working memory encoding and maintenance.

Whole-brain Fisher-r-to-Z correlation maps and associated scatterplots showing the relationship at the peak voxel, with age in years on the x-axes and oscillatory amplitude in pseudo-t units on the y-axes. (A-B) Theta oscillations became weaker with increasing age in posterior cerebellar cortices among females, but stronger with increasing age in anterior cerebellar cortices among males. (C) Alpha oscillations became stronger with increasing age in right superior temporal cortices among males, but weaker with increasing age among females.

*p < .05; $^{\mp}p$ < .01; **p < .005; $^{\mp\mp}p$ < .001.

Discussion:

In this study, we used high-density MEG to probe the relationship between chronological age and oscillatory activity supporting working memory, in a sample of 6-to-14-year-old youth. During encoding, we found that age was significantly associated with increased theta power in bilateral occipital cortices and decreased theta in regions of right cerebellar cortices that differed by sex. Additionally, during encoding, age was associated with stronger alpha oscillations (i.e., decreases in power) in left-lateralized language and executive function regions, such as the left prefrontal, supramarginal, and OTC. Interestingly, the opposite relationship was seen in the right prefrontal cortex, with alpha oscillations becoming weaker with increasing age. During the maintenance phase, alpha oscillations became stronger with increasing age across multiple cortical regions, including occipital, parietal, OTC, and prefrontal cortices. Additionally, in the right supramarginal cortex, males and females showed different developmental trajectories of alpha oscillations during the maintenance phase of working memory. Below, we discuss the implications of these results for our understanding of VWM processing during child and adolescent development.

First, our behavioral findings indicated that older youth performed significantly faster and more accurately than younger youth, which has been reported by previous studies of VWM in developing youth (*32, 51*). These behavioral results may be due to older youth employing more advanced strategies, or even a wider array of strategies, to encode and maintain the stimulus sets such that they could recognize whether the stimulus probe was in- or out-of-set quicker and with better precision. Alternatively, more advanced reading ability may contribute to faster and more accurate VWM processing. Future work is required to substantiate these hypotheses.

Regarding our neural data, we found that alpha oscillations during encoding became stronger with increased age in the left dorsal prefrontal, left supramarginal, and left OTC, and these effects extended into the maintenance phase in several brain regions, including the left frontal and left OTC. This aligns with, and extends, previous adult studies (*31, 45, 47*), which have reported left prefrontal and supramarginal alpha oscillations, beginning during encoding and lasting throughout most of the maintenance phase. This particular pattern of activity has been described within the framework of Baddeley's multicomponent working memory model (*20, 64*), where left prefrontal alpha oscillations may reflect activity of the central executive component, responsible for coordinating efforts of various neural regions and allocating attentional resources to relevant stimuli (*31, 42, 47*). Further, alpha oscillations in the left supramarginal gyrus have been proposed to reflect the activity of the phonological loop, engaging in subvocal rehearsal to refresh stimulus representations from memory decay (*31, 32, 42*). Surprisingly, our results also showed that alpha oscillations became weaker in right anterior prefrontal cortices with increased chronological age. These results may indicate increased cortical specialization for VWM processing, with less involvement of right hemispheric prefrontal cortices and increased activity in left hemispheric homologs being more specialized for verbal stimuli (*32, 45*).

The phonological loop is believed to permit short-term maintenance of verbal information via a phonological store that holds speech-related information for a very short time, after which sub-vocal rehearsal is initiated by articulatory control processes to refresh the contents of the phonological store (*20, 64*). Considering the significant association between age and alpha oscillations in the left supramarginal and OTC, in addition to those in the left prefrontal cortices, our results align with the development of a distributed VWM network. The left supramarginal gyrus has long been known as a critical hub for language processing, including phonological decoding and articulatory rehearsal

(*65-68*). Further, the OTC houses the visual word form area (*69*), an area central to visual processing during reading which has been shown to be preferentially activated in response to printed words as opposed to symbols or checkerboard patterns (*70*). Taking the extant adult MEG and fMRI working memory literature into account, the observed changes in alpha activity within this sample align with the maturation of integral components of the working memory network with increasing age, across males and females.

Properly encoding visual stimuli necessitates involvement of the early visual cortices, thus the increased bilateral occipital theta power with age may suggest maturation of early visual processing among older youth. Adult studies reporting increased occipital theta activity have suggested that it is associated with attentional exploration, as a necessary component of early visual processing (*71-75*). Increased theta activity during a visuospatial task has also been associated with increased age in a sample of youth (*76*). Beyond visual cortices, we also found sex-by-age interactions in theta oscillatory responses in the cerebellum, with males showing decreases with age in anterior regions of the right cerebellum, and females showing decreases with age in posterior cerebellar cortices. This may reflect the density of sex steroid receptors in the cerebellum, especially during this developmental stage (*77*). Previous work studying the cerebellum's functional role in working memory has suggested it aids in computing the difference between actual and intended phonological rehearsal, eventually updating communications to frontal cortices that will aid the phonological loop (*78*). At least one study has reported load-dependent increases in cerebellar activation, suggesting that it reflected increased input from prefrontal cortices that were involved in the articulatory control system of the phonological loop (*23*). Previous MEG studies have reported right cerebellar alpha oscillations during the maintenance phase of working memory in adults (*45, 46, 79*) and

sex differences in right cerebellar alpha power during maintenance in developing youth (*32*), emphasizing its importance for maintaining stimuli.

During maintenance, increased age was significantly associated with stronger alpha oscillations (i.e., more negative) in the right occipital and right parietal cortices, this finding was unexpected as the adult literature shows the opposite pattern (i.e., alpha inhibition) in parieto-occipital regions. Some have suggested that such alpha responses reflect the inhibition of visual pathways that acts to block visual input when there is a greater chance of memory decay (*31, 80-82*). Further, one analysis in adults focused on the time course of parieto-occipital alpha, and found that increased alpha power strongly dissipated during the final time bin before retrieval, which the authors suggested may reflect decreased inhibition as the processes needed for retrieval are initiated (*31*). In our sample, the majority of younger participants exhibited increased alpha power relative to baseline (i.e., alpha inhibition). Among the older youth participants, some displayed increased alpha power while others exhibited decreased alpha relative to baseline. We suggest that the older participants who displayed decreased alpha power across the time span of 800 ms preceding retrieval may have initiated their retrieval processing earlier, thus releasing their inhibitory processes early in the 800 ms imaging window. Being that this task was four-load, it is likely the older youths found this task to be less difficult and were able to release their inhibitory processing earlier. Future work should probe the effects of alpha power latency in parieto-occipital cortices and its relationship to behavioral performance.

Before closing, we must acknowledge a few limitations of our study. This analysis utilized data from only one time point, thus we were unable to make within-subjects conclusions about development. Further, because we did not find behavioral correlations with alpha or theta power in regions that exhibited significant associations with age, we

were unable to definitively say that patterns of change directly contributed to improved performance with age. Future studies would benefit from utilizing multiple time points in a longitudinal design, as this may offer a wider view of the developmental processes at play. Overall, with our use of high-density MEG and dynamic functional mapping, we have identified developmentally sensitive regions of a distributed network supporting working memory processing. We identified age-related changes in theta and alpha signatures of encoding and maintenance and provided a foundation for the further delineation of developmental changes in VWM-related oscillatory activity. While our findings were consistent with adult and developmental accounts, findings in youth as young as six years old have not been previously described, which therefore further extend our understanding of this critical cognitive function toward early childhood.

CHAPTER 2: GROWING TOGETHER: DYNAMIC CONNECTIVITY BETWEEN DEVELOPMENTALLY SENSITIVE REGIONS SERVING VERBAL WORKING MEMORY IN CHILDREN AND ADOLESCENTS

Introduction:

As children mature into adolescence, they experience improvements in working memory that facilitate learning and decision-making amidst changing social roles and environments. Working memory is the short-term retention of information and the executive processes supervising what information is retained (*20, 83, 84*). It begins with encoding, the initial perception and stimulus loading into memory stores. This is followed by a short maintenance period, the active rehearsal of information to be kept it in memory. The process ends with the retrieval of information from memory stores. Baddeley's tri-partite model posits that individuals utilize a phonological loop or visuospatial sketchpad to maintain different stimulus features and a central executive to govern attentional allocation (*20*). Studies aimed at identifying a "working memory network" have shown that the prefrontal cortex contributes to central executive operations by governing stimulus selection and executive control (*85-90*). Regions of the left temporal and inferior parietal cortices have been reliably associated with the phonological store and articulatory rehearsal components of the phonological loop (*91, 92*), and studies probing the visuospatial sketchpad have linked it to early visual cortices (*93*). Thus, working memory relies on communication between neural regions that have protracted developmental courses, driven by local synaptic pruning (*2*), white matter microstructural changes (*94, 95*), and strengthening of white matter pathways (*96, 97*).

So far, analyses probing verbal working memory (VWM) network maturation point to a variable developmental trajectory, with increasing and decreasing activation in key regions with age (*22, 35, 91, 98, 99*), reflecting how different areas "come online" during development. There is, however, significant left hemisphere lateralization for VWM in the

frontal and parietal lobes, and less default mode network activation with increased adolescent development (*100*). Oscillatory activity between neuronal populations is critical to the information transfer necessary for VWM (*26, 27, 101*) as it is an important mechanism for synchrony among distributed brain regions (*83*). Many adult studies characterizing the spectral dynamics supporting VWM have shown a decrease in alpha relative to baseline (i.e. stronger alpha) in bilateral occipital cortices that begins during encoding and moves into the left inferior parietal, temporal, and frontal cortices (*45, 46, 79*). This activity is sustained throughout maintenance and is suggested to reflect functional interactions for guiding and storing verbal information until retrieval (*31, 42*). During maintenance, studies also found an increase in alpha activity in parieto-occipital cortices, which is suggested to reflect attentional control, blocking out distractions from task-irrelevant stimuli (*80, 81*). On average, alpha activity during VWM in children and adolescents closely mirrors the distributed nature of activity in adults. The limited studies that have examined the effects of age on VWM alpha activity have found significant effects in left-lateralized temporal and parietal cortices, as well as bilateral occipital and frontal cortices (*32-34*). However, the functional connectivity between these regions is still being explored.

At the level of whole-brain networks, resting-state functional magnetic resonance imaging (fMRI) studies suggest that by age 7, network hubs once confined to sensory and motor regions shift to regions better equipped for mature integration of endogenous and exogenous mental processes (*96, 102*). From middle childhood to adulthood, short-range connections are weakened to support the segregation of neural information and long-range connections are strengthened to support information integration (*96*). This network development is also spectrally specific, with alpha and beta networks during working memory maintenance having short path lengths (*103*), and older adolescents exhibiting

more segregated alpha networks with weaker connections in cognitive control and attention networks at rest (*104*). With regard to functional connectivity, researchers have used fMRI to probe the impacts of age on functional connectivity during VWM. Finn et al. (*105*) used a longitudinal design to examine the development of hippocampal and prefrontal connectivity in adolescents. They found connectivity differences between mid to late adolescents, whereby hippocampal recruitment decreased, resulting in weaker hippocampal-prefrontal connectivity with age. In a later study of typically developing children and adolescents, van den Bosch et al. (*106*) found improved working memory performance with age and weaker functional connectivity with age between the left prefrontal, left parietal, and right cerebellar regions. However, this effect was no longer present when controlling for working memory performance. One study used MEG to examine how working memory networks develop and found a positive relationship between accuracy and average whole-brain alpha connectivity during maintenance (*107*). However, the analyses only focused on maintenance, in 6-year-old children, leaving the need to study connectivity during VWM encoding and maintenance across developmental years.

It is surprising that very few studies have looked to spectrally specific developmental patterns in functional connectivity between WM-related regions, during childhood and adolescence. Studying the dynamics of functional connectivity in typically developing youth may reveal developmental modifications occurring between specific cortical regions within the widely distributed working memory network. As the recruitment of a specific region changes with age, so will its communication with other necessary cortical areas. To this end we used phase coherence to quantify the level of functional connectivity between developmentally sensitive regions supporting VWM, which we identified in a previous analysis. Then, we probed whether functional connectivity scaled with age to elucidate

how these regions may be working together, or independently from one another, during development.

Methods:

Participants

As part of the Developmental Multimodal Imaging of Neurocognitive Dynamics study, 106 youth between the ages of 6 and 14 (*M*=10.07 years, *SD* = 2.53; 50 females; 11 left-handed) were recruited from the community. This is an NIH-supported project (R01-MH121101) utilizing an accelerated longitudinal design to study brain and cognitive development, but due to the accelerated nature of the study, 10-year-olds were not enrolled during the first year. This investigation uses data from the first year of the study, and a portion of the analyses was published elsewhere. All participants were typically developing primary English speakers without diagnosed psychiatric or neurological conditions, previous head trauma, learning disability, or non-removable ferromagnetic material (e.g., orthodontia). Written informed assent and consent were obtained from the child and the child's parent or legal guardian, after a complete description of the study. All procedures were completed at the University of Nebraska Medical Center and approved by the University of Nebraska Medical Center Institutional Review Board.

MEG Experimental Paradigm

Participants completed a modified Sternberg VWM task similar to those used in several previous studies of adults (*31, 43, 46, 52, 53*) and youths (*32*). Participants rested their right hand on a custom five-finger button response pad directly connected to the MEG system so that each button press sent a TTL pulse to the acquisition computer in real-time, enabling behavioral responses to be temporally synced with the MEG data. Accuracy and reaction time were calculated offline. Participants were shown a centrally presented

fixation cross embedded in a 5x5 grid for 1,000 ms (i.e., baseline period). An array of four consonants then appeared at fixed locations within the grid for 2,000 ms (i.e., encoding period). The letters disappeared from the array leaving an empty grid shown for 2,000 ms (i.e., maintenance period), during which participants had to maintain the encoded letters from the previous phase. A probe letter then appeared on the grid for 1,500 ms (i.e., retrieval period), and participants were instructed to respond with their right index if the probe letter was found in the previous array of letters or with their middle finger if it was not. Participants completed 128 trials, split equally and pseudorandomized between in- and out-of-set trials, for a total run time of about 15 minutes (see Figure 6). Visual stimuli were presented using the E-Prime 2.0 software (Psychology Software Tools, Pittsburgh, PA), and back-projected onto a semi-translucent nonmagnetic screen at an approximate distance of 1.07 m, using a Panasonic PT-D7700U-K model DLP projector with a refresh rate of 60 Hz and a contrast ratio of 4000:1.

MEG Data Acquisition

Participants sat in a nonmagnetic chair within a one-layer magnetically shielded room with active shielding engaged during MEG recording. Neuromagnetic responses were sampled continuously at 1 kHz with an acquisition bandwidth of 0.1 – 330 Hz using an MEG system with 306 magnetic sensors (MEGIN, Helsinki, Finland). MEG data from each subject were individually corrected for head motion (MaxFilter v2.2; MEGIN) and subjected to noise reduction using the signal space separation method with a temporal extension (*54, 55*).

Structural MRI Data Acquisition and MEG Co-registration

A 3T Siemens Prisma scanner equipped with a 32-channel head coil was used to collect high-resolution structural T1-weighted MRI data from each participant (TR: 24.0 ms; TE: 1.96 ms: field of view: 256 mm; slice thickness: 1 mm with no gap; in-plane

resolution: 1.0 x 1.0 mm). Structural volumes were aligned parallel to the anterior and posterior commissures and transformed into standardized space. Each participant's MEG data were co-registered with their MRI data using BESA MRI (Version 2.0). After source imaging (beamformer), each subject's functional images were also transformed into standardized space using the transform previously applied to the structural MRI volume, and spatially resampled.

MEG Time-Frequency Decomposition and Statistical Analysis

Cardiac and ocular artifacts were visually inspected and removed from the data using signal-space projection, which was accounted for during source reconstruction (*57*). The continuous magnetic time series was divided into 5900 ms epochs, with stimulus presentation (i.e., 5x5 grid containing four consonants) defined as 0 ms and the baseline defined as the -400 to 0 ms time window (i.e., fixation period; Figure 1). Only correct trials were used for analysis. Epochs containing artifacts were rejected based on a fixed threshold method, which was supplemented with visual inspection. Briefly, the distributions of amplitude and gradient values per participant were computed using all correct trials, and the highest amplitude/gradient trials relative to the total distribution were excluded. Notably, individual thresholds were set for each participant for both amplitude (*M* = 2145.88 fT/cm, *SD* = 909.0) and gradient (*M* = 539.34 fT/(cm*ms), *SD* = 258.4) due to differences among individuals in head size and sensor proximity, which strongly affect MEG signal amplitude. Note that an average of 87.20 (SD: 12.1) trials per participant remained for further analysis and the number of accepted trials was not significantly correlated with age and did not differ between sexes.

Artifact-free epochs were then transformed into the time-frequency domain using complex demodulation with a resolution of 1.0 Hz and 50 ms (*58, 59*). The resulting spectral power estimations per sensor were averaged over trials to generate time-

frequency plots of mean spectral density. These sensor-level data were then normalized per frequency bin using the mean power during the –400 to 0 ms baseline period. The specific time-frequency windows used for imaging were determined by statistical analysis of the sensor-level spectrograms across the entire array of gradiometers. Each data point in the spectrogram was initially evaluated using a mass univariate approach based on the general linear model. To reduce the risk of false-positive results while maintaining reasonable sensitivity, a two-stage procedure was followed to control for Type 1 error. In the first stage, paired-samples t-tests against baseline were conducted on each data point and the output spectrogram of t-values was threshold at $p < .05$ to define time-frequency bins containing potentially significant oscillatory deviations across all participants. In stage two, time-frequency bins that survived the threshold were clustered with temporally and/or spectrally neighboring bins that were also below the ($p < .05$) threshold, and a cluster value was derived by summing all of the t-values of all data points in the cluster. Nonparametric permutation testing was then used to derive a distribution of cluster-values, and the significance level of the observed clusters (from stage one) was tested directly using this distribution (*60, 61*). For each comparison, 10,000 permutations were computed to build a distribution of cluster values. Based on these analyses, time-frequency windows that contained a significant oscillatory event based on permutation testing were subjected to the beamforming analysis.

MEG Source Imaging and Statistics

Cortical oscillatory activity was imaged through an extension of the linearly constrained minimum variance vector beamformer (*62, 63*) using the Brain Electrical Source Analysis (BESA 7.0) software. This approach, commonly referred to as DICS or dynamic imaging of coherent sources, applies spatial filters to time-frequency sensor data to calculate voxel-wise source power for the entire brain volume. The single images are

derived from the cross-spectral densities of all combinations of MEG gradiometers averaged over the time-frequency range of interest, and the solution of the forward problem for each location on a 4.0 × 4.0 × 4.0 mm grid specified by input voxel space. Following convention, we computed noise-normalized, source power per voxel in each participant using active (i.e., task) and passive (i.e., baseline) periods of equal duration and bandwidth. Such images are typically referred to as pseudo-*t* maps, with units (pseudo-*t*) that reflect noise-normalized power differences (i.e., active vs. passive) per voxel. This generated participant-level pseudo-*t* maps for each time-frequency-specific response identified in the sensor-level permutation analysis, which was then transformed into standardized space using the transform previously applied to the structural MRI volume and spatially resampled.

Resultant pseudo-*t* maps were averaged within participants across the time windows used to image neural activity during encoding and maintenance periods, separately. The averaged source maps did not include maps representative of time windows spanning two different phases of the task (e.g., encoding and maintenance). Developmental associations with neural activity were examined via whole-brain voxel-wise correlations with chronological age across the entire sample. To account for multiple comparisons, a significance threshold of $p < .005$ was used in all statistical maps to identify significant clusters, in addition to a cluster threshold of 8 contiguous voxels.

Functional Connectivity Analysis

To analyze the functional connectivity between peak voxels identified in our whole brain correlations with age, we computed the phase-locking value (PLV). The PLV reflects the intertrial variability of the phase relationship between pairs of brain regions as a function of time. Values close to 1 indicate strong synchronicity (connectivity), or phase-locking, between the two voxel time series within the specific time-frequency bin across

trials. Values close to 0 indicate greater phase variability between the two signals, or low connectivity between the two regions. Using the method described in Lachaux et al. (*108*), the mean PLV was extracted across the time windows used to beamform the 8-12 Hz alpha response (i.e., 400 – 2,000 ms for encoding and 3,100 – 3,900 ms for maintenance), and baseline-corrected these values. Using a full factorial analysis to probe developmental effects on functional connectivity, we probed the effects of sex, age, and the age-by-sex interactive effect on average PLV for each pair of brain regions.

Results:

Demographic and Behavioral Results

Demographic and behavioral results for this sample are reported in a previously published analysis. Briefly, 15 participants were excluded for accuracy less than 60%, leaving 91 participants in the final behavioral analysis. Participants were between 6 and 14 years old (M = 10.34, SD = 2.48; 42 females; 8 left-handed), and age did not significantly differ by sex (t(89) = -.35, p = .73). Participants had mean accuracy of 84.07% (SD = 10.46) and mean reaction time of 1204.78 ms (SD = 264.38). Accuracy was significantly, positively, correlated with age (r = .61, p < .001) but did not significantly differ between sex (t(89) = .58, p = .56). Reaction time was significantly, negatively, correlated

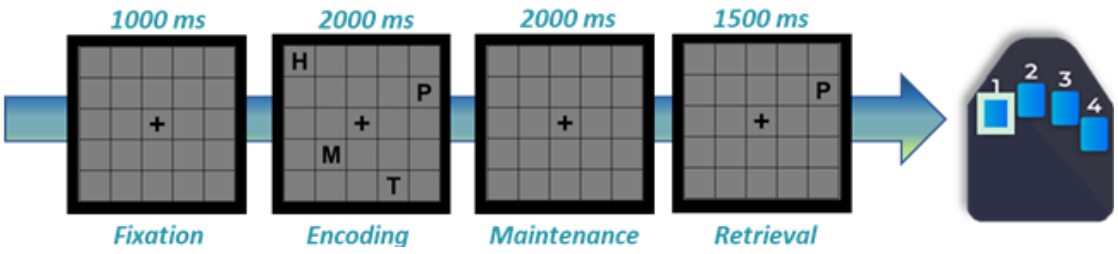

Figure 6: Modified Sternberg VWM task and behavior.

An example trial of the modified Sternberg working memory task along with the corresponding correct response shown on the button response pad in blue.

with age (r = -.64, p < .001) and did not significantly differ between sex (t(89) = 1.26, p = .21).

MEG Sensor-Level and Source-Level Results

Statistical examination of sensor-level time-frequency spectrograms showed two responses during the encoding period. A significant decrease in alpha (8-12 Hz) began 400 ms after encoding onset and extended until 2000 ms. During the maintenance period there was a strong increase in alpha activity (8-12 Hz), which began at 3,100 ms and lasted until 3,900 ms (p < 0.0001, permutation corrected; Figure 7). These alpha responses were divided into 400 ms non-overlapping time bins, with source reconstruction performed on the resultant time-frequency windows of interest.

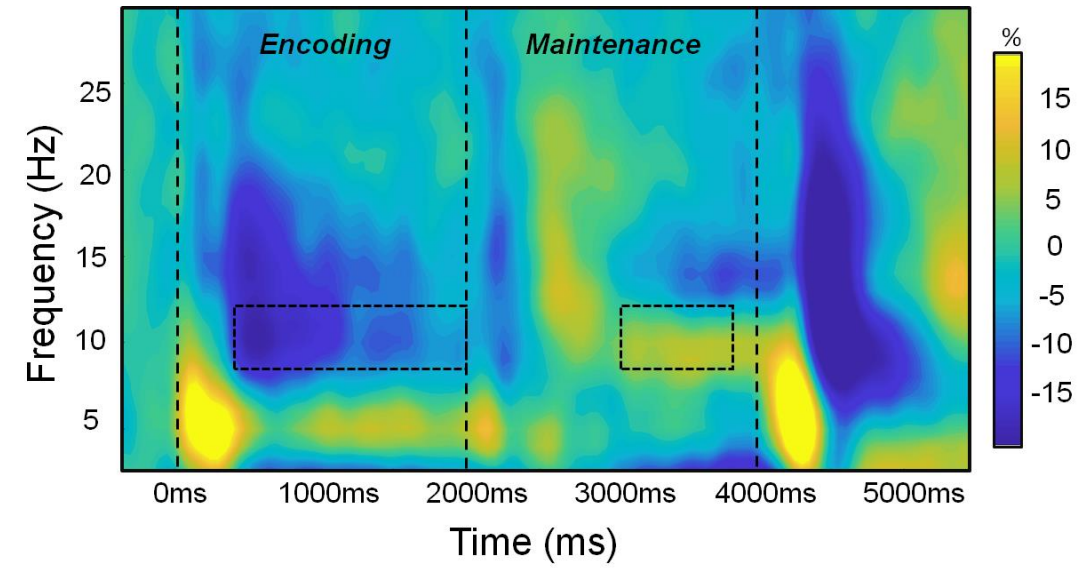

Figure 7: Grand-averaged MEG sensor-level spectrogram.

Grand-averaged time-frequency spectrogram taken from a representative sensor with time denoted on the x-axis (0.0 s = encoding onset) and frequency (Hz) is denoted on the y-axis. Time-frequency windows that were used for source estimation are denoted by the dashed black boxes. The spectrogram is shown in percent power change from baseline, with the color scale shown to the right of the spectrogram.

Ten participants were removed for having noisy MEG source-level data within the encoding time-frequency window (8-12 Hz, 400 – 2,000 ms), and 16 participants were removed for noisy MEG source-level data within the maintenance time-frequency window

(8-12 Hz, 3,100 – 3,900 ms). Therefore, the final sample analyzed at the source level consisted of 81 participants for the encoding phase and 75 participants for the maintenance phase. Average beamformer images across all participants revealed that the alpha response during encoding began in bilateral occipital regions and extended anteriorly to include left temporal regions as encoding progressed. During maintenance, increases in alpha (8-12 Hz) were mainly seen bilaterally in inferior-occipital cortices.

Developmentally Sensitive Neural Regions and Effects of Functional Connectivity

Whole-brain, voxel-wise correlations indicated that during encoding, with increasing age alpha (8-12 Hz) oscillations became stronger (i.e., more negative) in left dorsal prefrontal (left dlPFC; r = -.36, p < .001), supramarginal (r = -.55, p < .001), and occipito-temporal cortices (OTC; r = -.34, p < .005). Conversely, alpha oscillations during encoding became weaker with age in the anterior right prefrontal cortex (right PFC; r = .44, p < .001). There was an age-by-sex interactive effect on right PFC – left OTC phase-locking (p = .025; Figure 8), and the directionality indicated this trend was negative for young females but positive for all other participants. However, while this interactive effect was significant, post-hoc correlation analysis showed no significant correlation between age and right PFC – left OTC phase-locking within the four age-by-sex groups. Also, during encoding, there was a significant effect of age on left frontal – supramarginal phase-locking, controlling for sex (p = .001; Figure 9). The directionality of the simple slope indicated that older participants exhibited stronger phase-locking than younger participants.

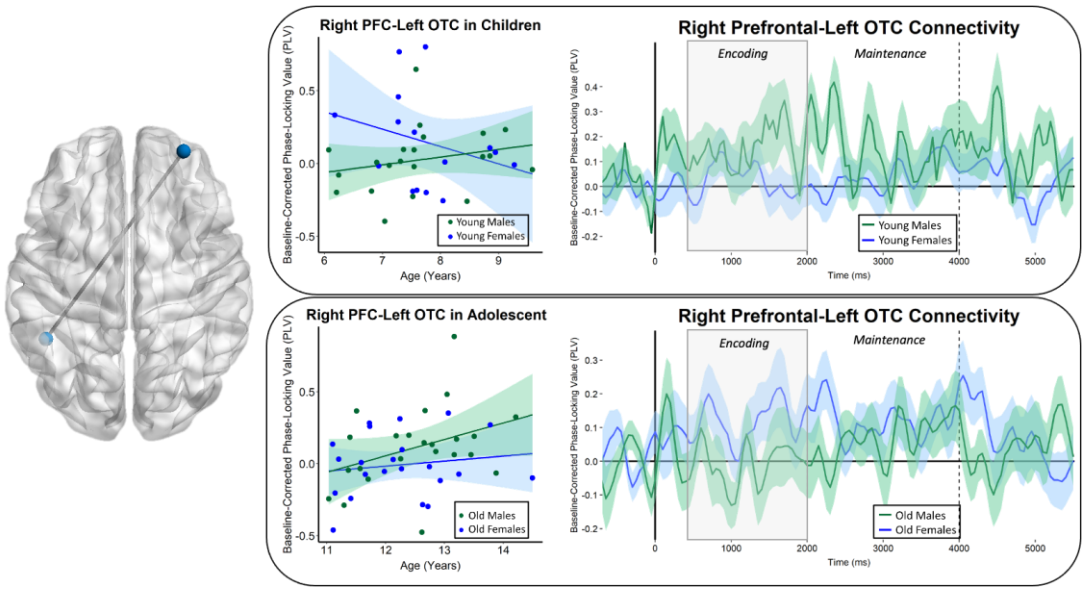

Figure 9: Connectivity time course for the right PFC-left OTC regions.

(Left) Blue nodes denote the location of the right PFC and left OTC clusters that exhibited significant whole-brain correlation between age and alpha (8-12 Hz) oscillatory activity. (Middle) Average baseline-corrected phase-locking-value for connectivity between the right prefrontal cortex (PFC) – left occipitotemporal cortex (OTC) is shown on the y-axis, with age in years on the x-axis. (Right) The connectivity time course for 6-9-year-olds is shown above and the time course for 11-14-year-olds is shown below, with males in green and females in blue.

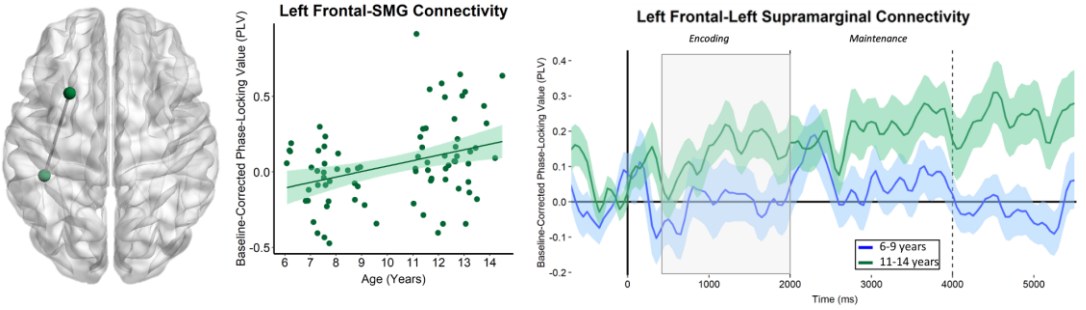

Figure 8: Connectivity time course for the left frontal-left supramarginal regions.

(Left) Green nodes denote the location of the left frontal and left supramarginal clusters that exhibited significant whole-brain correlation between age and alpha (8-12 Hz) oscillatory activity. (Middle) Average baseline-corrected phase-locking-value for connectivity between the left frontal cortex – left supramarginal gyrus is shown on the y-axis, with age in years on the x-axis. (Right) The connectivity time course for 6-9-year-olds is shown in blue and the time course for 11-14-year-olds is shown in green. As seen in the grey box, and the scatterplot, connectivity among adolescents was significantly greater than connectivity among children during encoding.

During maintenance (3100 – 3900 ms), alpha oscillations became stronger with age within the right occipital cortices (r = -.36, p < .005), right parietal cortices (r = -.37, p < .001), left prefrontal cortices (r = -.38, p < .005), and left OTC (r = -.38, p < .001). During

maintenance, there was a significant effect of age on left PFC – right occipital phase-locking (p = .006; Figure 10), with the directionality indicating that phase-locking was weaker among older youth than younger youth. Age also had a significant effect on left OTC – right parietal phase-locking (p = .003; Figure 11), and the directionality indicated that older participants had stronger phase-locking than younger participants, above and beyond the effects of sex.

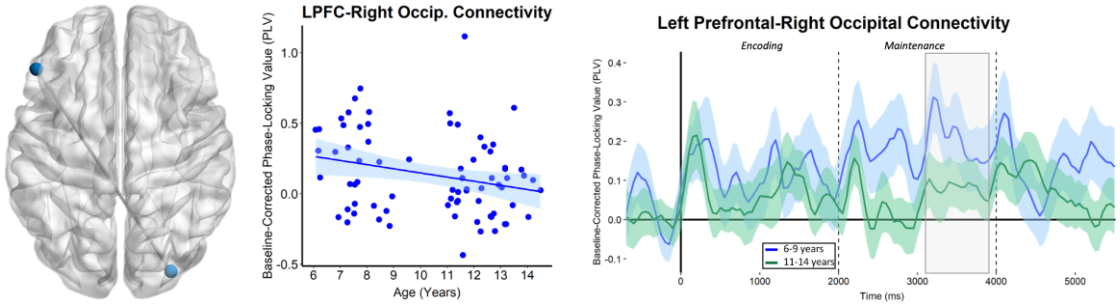

Figure 10: Connectivity time course for the left prefrontal-right parietal regions.

(Left) Blue nodes denote the location of the left prefrontal (PFC) and right occipital (Occip.) clusters that exhibited significant whole-brain correlation between age and alpha (8-12 Hz) oscillatory activity. (Middle) Average baseline-corrected phase-locking-value for connectivity between the left PFC – right occipital cortex is shown on the y-axis, with age in years on the x-axis. (Right) The connectivity time course for 6-9-year-olds is shown in blue and the time course for 11-14-year-olds is shown in green. As seen in the grey box, and the scatterplot, connectivity among adolescents was significantly greater than connectivity among children during maintenance.

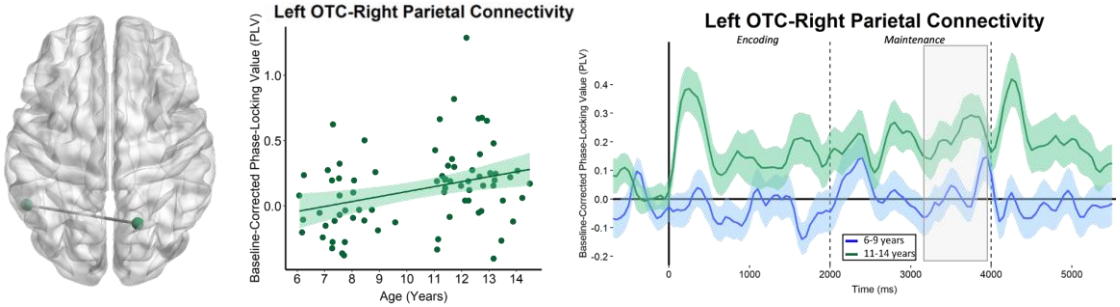

Figure 11: Connectivity time course for the left frontal-left supramarginal regions.

(Left) Green nodes denote the location of the left OTC and right parietal clusters that exhibited significant whole-brain correlation between age and alpha (8-12 Hz) oscillatory activity. (Middle) Average baseline-corrected phase-locking-value for connectivity between the left OTC – right parietal cortex is shown on the y-axis, with age in years on the x-axis. (Right) The connectivity time course for 6-9-year-olds is shown in blue and the time course for 11-14-year-olds is shown in green. As seen in the grey box, and the scatterplot, connectivity among adolescents was significantly greater than connectivity among children during maintenance.

Discussion:

In a previous analysis, we reported age-related changes of alpha (8-12 Hz) oscillatory activity during VWM encoding and maintenance in bilateral frontal cortices, temporal and parietal regions of the left-lateralized language network, and right occipital and parietal cortices. In this analysis, we used phase-locking values to probe age-related alterations in the functional connectivity between these regions. During encoding, left PFC-supramarginal PLV increased with age. Also, during encoding, right PFC-left OTC PLV was significantly altered by an interactive effect between age and sex. Males, in both the child and adolescent groups and adolescent females, exhibited a trend of increasing connectivity, while female children exhibited an opposite trend. However, post-hoc analysis revealed that none of the individual relationships were significant. In maintenance, results showed adolescents had weaker left PFC-right occipital connectivity than children, but stronger left OTC-right parietal connectivity. This study furthers the previous report on the typical development of oscillatory power serving VWM, by detailing how the functional connectivity within this network of developmentally sensitive regions dynamically change with age.

Gradual decreases in grey matter thickness and increases in myelination that traverse the parietal, frontal, and temporal cortices from childhood to adolescence equip youth with the structural framework to meet the increasing demands of cognitive and attentional control as they mature. With a previous study showing that increased structural connectivity between supramarginal and prefrontal regions during development is positively related to working memory span (*40*), it appears that the increased strength of left PFC-supramarginal functional connectivity with age allows for higher-fidelity phonological encoding, possibly making stimulus representations during maintenance much less subject to decay. Although not verbal in nature, studies on visuospatial working

memory have suggested that task-irrelevant distractors can be better ignored by modulating cortical activity early on (*109*), so that information is better maintained in mind and working memory capacity is not overloaded (*110*).

Sato et al. (*107*) compared alpha whole-brain connectivity during working memory for correct and incorrect trials and found that connectivity in frontoparietal cortices peaked soon after encoding but only remained stable through maintenance on correct trials. Of note, their results also showed that children exhibited stronger frontotemporal connectivity than frontoparietal connectivity, suggesting that phonological encoding was probably the main support for accurate working memory processing. While this analysis did not probe developmental changes in connectivity between regions of the left temporal cortex that contribute to the phonological loop component of Baddeley's model (i.e. superior temporal sulcus and anterior temporal cortex), future work should probe developmental trends using non-directed forms of connectivity with either the left supramarginal or left prefrontal cortices as seed regions. This may allow a deeper understanding of the age-related changes in oscillatory information transfer within the left-lateralized language regions, specifically during VWM processing.

During encoding, a significant interaction emerged in the phase-locking between the right frontal and left OTC, suggesting that its relationship with age differed by sex. Post-hoc testing showed general, non-significant trends, whereby PLV seemed to decrease with age among younger females but increased with age for all other participants (i.e., 6 – 9-year-old males and 11-14-year-old males and females). In a study of typically-developing youth, Embury et al. (*32*) found that during encoding female youth exhibited a stronger alpha decrease relative to baseline within right prefrontal cortices. They likened the recruitment of this right homologue region to that of healthy aging, proposing that it may have a positive effect on VWM performance (*45*). Studies in children learning to read

have found that reading acquisition progressively modifies the functionality of the left lateral occipitotemporal sulcus, such that it develops specificity for “the abstract sequence of letters” that make up words, in a strictly visual and prelexical manner (*69, 70*). Thus, our results demonstrating functional connectivity between the right prefrontal cortex and the left OTC may point to functionality supporting the prelexical or visual encoding of the letter stimuli; a means of spatially oriented attentional control for letter encoding. As participants are encoding the letters, they may be encoding the spatial location of the letters within the grid to bolster the stimulus representations that will be maintained.

Although the OTC has been primarily identified as a main contributor to word-form in the language and reading network, some studies suggest that the left OTC is at an integration point between the language network and the fronto-parietal attention network (*111-113*). One study reported that during a reading task, increased connectivity between the ventral OTC and the intraparietal sulcus node of the frontoparietal attention network positively predicted performance on visuospatial neuropsychological tests (*114*). The developmental effects on the left OTC’s connectivity with the right PFC during encoding, and the right parietal cortex during maintenance, align with its suggested role in the frontoparietal attention network. Thus, it’s conceivable that during encoding, the left OTC-right PFC functional connectivity supports spatial aspects of letter encoding, but during maintenance left OTC-right parietal cortex connectivity helps maintain the spatial location of the letters.

In our previous analysis, we report that older youth exhibited stronger alpha activity (i.e. more negative) during maintenance in the right occipital cortices. Because adult studies have suggested that occipital alpha during maintenance is weaker (i.e., more positive) as a mechanism of blocking task-irrelevant distractors or meeting increased attentional demands (*82, 115-117*), we hypothesized that older youth might exhibit

stronger alpha towards the end of maintenance because they are releasing inhibitory processes and initiating retrieval earlier. This hypothesis aligns with our results of decreased functional connectivity between this region and the left prefrontal cortex with age, showing that older youth exhibit less functional integration between stimulus selection and visual attention areas. As youth advance through development from childhood to adolescence, they may mature from simply visually representing the letter stimuli to more complex spatial representations integrating the location of the stimuli with the prelexical visual representation. Future research should examine the directionality of these functional connections to determine the flow of information during encoding and maintenance. It would be interesting to analyze whether connectivity during maintenance is dependent on connectivity strength during encoding, or whether top-down influences on attentional control during maintenance bias the cognitive representations of visual stimuli away from visual regions and towards higher-order association cortices.

While our analysis results offer tremendous insight into the age-related alterations of functional connectivity between developmentally sensitive regions serving VWM, there some limitations that should be considered for future studies. While the focus of this investigation was alpha oscillatory activity in the 8-12 Hz frequency range, oscillatory activity in higher alpha (e.g., 9-14 Hz) and theta frequencies are also sensitive to age-related changes in distinct cortical regions. Studies should probe the relationship between chronological age and functional connectivity between developmentally-sensitive regions within other frequency bands to provide more insight. Additionally, studies have shown robust associations between cortical structure during development, with fewer showing functional relationships. Analyses perturbing relationships between endogenous hormone levels and functional connectivity during the pubertal transition years would be immensely beneficial to the field of developmental neuroscience for both typical development and

implications for psychopathology. Broadly, our results suggest that communication between developmentally sensitive cortical regions supporting VWM scales with age, in a manner that optimally integrates information transfer between phonological and attention-related systems. It also suggests that both long and short-range communication, between and within hemispheres, may be integral to the oscillatory development of VWM with age.

CHAPTER 3: EFFECTS OF ENDOGENOUS TESTOSTERONE ON OSCILLATORY ACTIVITY DURING VERBAL WORKING MEMORY IN YOUTH

Introduction:

Working memory (WM) is the cognitive ability to transiently maintain information in memory for later utilization and increases in capacity from infancy to young adulthood (*17, 21, 118, 119*). The cortical regions supporting WM, such as the parietal and prefrontal cortices (*22, 105, 120, 121*), undergo immense structural change during childhood and adolescence. Numerous investigations have probed the developmental effects of age on neural activity contributing to WM processing and have reported findings across a distributed cortical network (*24, 25, 32, 33, 35, 91, 100, 105, 119, 121-127*). In general, neuroimaging studies have shown that certain working memory network hubs (i.e., performance-enhancing regions) are more strongly recruited as a function of development, while other regions appear to become less involved in such processes. Still, the timing and other specifics of such development remain incompletely understood. One critical barrier to progress in this area has been the high degree of individual variability, as chronological age and developmental stage are more tightly coupled in some children relative to others. Thus, we propose that using hormones as a marker of developmental stage may offer unique insight over chronological age alone. Puberty is the developmental period when secondary sex characteristics emerge, leading to changes in self-perception and social experiences. It is initiated by adrenarche, the process by which the adrenal cortex significantly increases testosterone production (*5, 6, 128*). Adrenarche can begin as early as six years old, well before secondary sex characteristics emerge. But, in addition to changes in metabolic and growth rates, adrenarche also ushers in changes to neural systems, leading to downstream effects on cortical maturation patterns (*5, 12, 129*).

Much of our knowledge regarding the mechanism of testosterone's effects comes from animal models. Studies in rats have shown that neuron exposure to increased levels

of testosterone is associated with increased neuronal spine density in the amygdala and hippocampal pyramidal neurons (*130*), with mice studies showing that gonadectomy leads to morphological changes in dendritic spines of hippocampal pyramidal neurons (*11*). Overall, studies point to testosterone's key role in neuronal plasticity (*131-133*). However, researchers are also beginning to see that the effects of pubertal hormones on neural structure and function might be more nuanced in humans with region- or circuit-specificity, interactions with sex, and both increases and decreases in plasticity (*12, 134*). For example, Bramen et al. (*135*) reported significant effects of testosterone on the cortical thickness of regions known to be involved in working memory processing. Males with higher testosterone had greater cortical thickness in cuneate, lingual, and frontal cortices, whereas females had less cortical thickness. In inferior parietal and middle temporal cortices, however, females showed positive relationships between testosterone and cortical thickness while males did not. Another investigation showed smaller anterior cingulate grey matter volumes among males with higher testosterone but no significant relationships in females (*136*).

Studies using magnetoencephalography (MEG) have built upon these structural studies and shown that testosterone's effects on neural oscillatory activity differ from the effects of chronological age in spatial and spectral specificity. For example, when examining gamma activity subserving visuospatial processing Fung et al. (*137*) found that females with higher testosterone exhibited stronger gamma activity in the right temporal-parietal junction (TPJ) while high testosterone males exhibited stronger gamma activity in the right insula. They proposed that these results reveal differential maturational patterns in stimulus detection networks, as the TPJ and insula are both critical for facilitating bottom-up processing. When age effects were considered, significant relationships were found between chronological age and alpha activity in the right medial prefrontal, precentral, and cingulate cortices. Thus, effects of testosterone and age not only differed

in spatial specificity but spectral specificity. Other studies have found testosterone to mediate the relationship between age and the beta oscillations serving motor control (*138*) and for sensorimotor processing (*139*) in primary motor cortices. Furthermore, testosterone has been found to modulate spontaneous delta, beta, and gamma oscillatory activity in developing youth, with relationships that differed by sex (*140*).

Thus, considerable data suggests that testosterone significantly affects cortical structure and neural oscillatory activity during development, but no work has probed testosterone's relationship with working memory processing, which is surprising given the broad importance of working memory to overall cognitive function, and its relationship with social and emotional processing. As noted above, several previous studies have reported robust changes in the neural oscillations serving working memory with increases in chronological age (*32, 33, 127*), which to at least some degree were likely driven by puberty related changes in endogenous testosterone. By deriving salivary measures of testosterone, we hope to delineate its effects on the neural oscillations supporting working memory processing in a cross-sectional sample of developing youth. Importantly, by examining a young sample of 6-14-year-olds we will be able to capture the beginning of the adrenarche process. To this end, we used a modified Sternberg verbal working memory (VWM) task during MEG and the resultant neural responses were time-frequency transformed and imaged using a beamforming approach. We used a whole-brain voxel-wise analysis to assess the main effects of testosterone, and possible interactive effects with sex, controlling for the effects of age. Based on the previous literature, we hypothesized that we would see significant effects of testosterone on alpha and theta oscillatory activity, in different cortical regions supporting working memory, with some of these effects differing by sex.

Methods:

Participants

Eighty-nine participants ages 6-14 years old completed a modified Sternberg VWM task and provided saliva samples for hormone analysis as part of the NIH-supported Developmental Multimodal Imaging of Neurocognitive Dynamics study (R01-MH121101). This project employed an accelerated longitudinal design to investigate brain and cognitive development, and the current investigation utilizes cross-sectional data collected exclusively during year one (of note, due to the accelerated longitudinal design of the study, 10-year-olds were not enrolled). Participants were recruited from the community and were all typically developing primary English speakers without diagnosed psychiatric or neurological conditions, previous head trauma, learning disability, or non-removable ferromagnetic material (e.g., orthodonture). After a complete description of the study, written informed assent and consent were obtained from the child and the child's parent or legal guardian, respectively. All procedures were completed at the University of Nebraska Medical Center and approved by the University of Nebraska Medical Center Institutional Review Board.

Salivary Hormone Collection and Analyis

Participants were instructed to refrain from chewing gum and consuming any foods or liquids for at least one hour before providing saliva samples. All saliva samples were collected on average in the afternoon (*M* = 15:31 hr, *SD* = 2:48 hr), and participants were instructed to passively drool into an Oragene DISCOVER (OGR-500; www.dnagenotek.com) collection tube until liquid saliva exceeded the fill line indicated on the tube, which was 2.0 mL. Before the release of the protease inhibitors for long-term storage, a single-channel pipette was used to extract 0.5 mL from the collection tube and placed in a -20° C freezer for storage. All samples were assayed with duplicate testing

using a commercially available assay kit for salivary testosterone (Salimetrics EIA High Sensitivity Salivary Testosterone Kit; www.salimetrics.com). The assay kit had a sensitivity of 0.67 pg/mL, with a range of 6.1 – 600.0 pg/mL. The intra and inter-assay coefficients of variation were 5.04% and 3.31%, respectively. The arithmetic means of the duplicate tests exhibited a non-normal distribution, thus values were natural log-transformed (skewness = -.75, kurtosis = 1.45).

MEG Experimental Paradigm

Participants completed a modified Sternberg VWM task similar to those used in several previous studies of adults (*31, 43, 46, 52, 53*) and youths (*32, 127*). Participants rested their right hand on a custom five-finger button response pad directly connected to the MEG system so that each button press sent a TTL pulse to the acquisition computer in real time, enabling behavioral responses to be temporally synced with the MEG data. Accuracy and reaction time were calculated offline. Participants were shown a centrally presented fixation cross embedded in a 5x5 grid for 1,000 ms (i.e., baseline period). Four consonants appeared at fixed locations within the grid for 2,000 ms (i.e., encoding period). The letters disappeared from the array leaving an empty grid shown for 2,000 ms (i.e., maintenance period), during which participants had to maintain the encoded letters from the previous phase. A probe letter appeared in the grid for 1,500 ms (i.e., retrieval period), and participants were instructed to respond with their right index if the probe letter was found in the previous array of letters or with their middle finger if it was not. Participants completed 128 trials, split equally and pseudorandomized between in- and out-of-set trials, for a total run time of about 15 minutes (see Figure 12). Visual stimuli were presented using the E-Prime 2.0 software (Psychology Software Tools, Pittsburgh, PA), and back-projected onto a semi-translucent nonmagnetic screen at an approximate distance of 1.07 m, using a Panasonic PT-D7700U-K model DLP projector with a refresh rate of 60 Hz and a contrast ratio of 4000:1.

MEG Data Acquisition

Participants sat in a nonmagnetic chair within a one-layer magnetically shielded room with active shielding engaged during MEG recording. Neuromagnetic responses were sampled continuously at 1 kHz with an acquisition bandwidth of 0.1 – 330 Hz using an MEG system with 306 magnetic sensors (MEGIN, Helsinki, Finland). MEG data from each subject were individually corrected for head motion (MaxFilter v2.2; MEGIN) and subjected to noise reduction using the signal space separation method with a temporal extension (*54, 55*).

Structural MRI Data Acquisition and MEG Co-registration

A 3T Siemens Prisma scanner equipped with a 32-channel head coil was used to collect high-resolution structural T1-weighted MRI data from each participant (TR: 24.0 ms; TE: 1.96 ms: field of view: 256 mm; slice thickness: 1 mm with no gap; in-plane resolution: 1.0 x 1.0 mm). Structural volumes were aligned parallel to the anterior and posterior commissures and transformed into standardized space. Each participant's MEG data were co-registered with their MRI data using BESA MRI (Version 2.0). After source imaging (beamformer), each subject's functional images were also transformed into standardized space using the transform previously applied to the structural MRI volume, and spatially resampled.

MEG Time-Frequency Decomposition and Statistical Analysis

Cardiac and ocular artifacts were visually inspected and removed from the data using signal-space projection, which was accounted for during source reconstruction (*57*). The continuous magnetic time series was divided into 5,900 ms epochs, with stimulus presentation (i.e., 5x5 grid containing four consonants) defined as 0 ms and the baseline defined as the -400 to 0 ms time window (i.e., fixation period; Figure 1). Only correct trials were used for analysis. Epochs containing artifacts were rejected based on a fixed threshold method, supplemented with visual inspection. Briefly, the distributions of

amplitude and gradient values per participant were computed using all correct trials, and the highest amplitude/gradient trials relative to the total distribution were excluded. Notably, individual thresholds were set for each participant for both amplitude (*M* = 2228.93 fT/cm, *SD* = 983.1) and gradient (*M* = 553.43 fT/(cm*ms), *SD* = 251.9) due to differences in head size and sensor proximity among individuals, which strongly affect MEG signal amplitude. An average of 87.06 (SD: 12.2) trials per participant remained for further analysis.

Artifact-free epochs were then transformed into the time-frequency domain using complex demodulation with a resolution of 1.0 Hz and 50 ms (*58, 59*). The resulting spectral power estimations per sensor were averaged over trials to generate time-frequency plots of mean spectral density. These sensor-level data were then normalized per frequency bin using the mean power during the –400 to 0 ms baseline period. The specific time-frequency windows used for imaging were determined by statistical analysis of the sensor-level spectrograms across the entire array of gradiometers. Each data point in the spectrogram was initially evaluated using a mass univariate approach based on the general linear model. To reduce the risk of false-positive results while maintaining reasonable sensitivity, a two-stage procedure was followed to control for Type 1 error. In the first stage, paired-sample t-tests against baseline were conducted on each data point and the output spectrogram of t-values was threshold at $p < .05$ to define time-frequency bins containing potentially significant oscillatory deviations across all participants. In stage two, time-frequency bins that survived the threshold were clustered with temporally and/or spectrally neighboring bins that were also below the ($p < .05$) threshold, and a cluster value was derived by summing all the t-values of all data points in the cluster. Nonparametric permutation testing was then used to derive a distribution of cluster-values, and the significance level of the observed clusters (from stage one) was tested directly using this distribution (*60, 61*). For each comparison, 10,000 permutations were computed

to build a distribution of cluster values. Based on these analyses, time-frequency windows that contained a significant oscillatory event relative to the permutation testing null were subjected to the beamforming analysis.

MEG Source Imaging and Statistics

Cortical oscillatory activity was imaged through an extension of the linearly constrained minimum variance vector beamformer (*62, 63*) using the Brain Electrical Source Analysis (BESA 7.0) software. This approach, commonly referred to as dynamic imaging of coherent sources (DICS), applies spatial filters to time-frequency sensor data to calculate voxel-wise source power for the entire brain volume. The single images are derived from the cross-spectral densities of all combinations of MEG gradiometers averaged over the time-frequency range of interest, and the solution of the forward problem for each location on a 4.0 $\times$ 4.0 $\times$ 4.0 mm grid specified by input voxel space. Following convention, we computed noise-normalized, source power per voxel in each participant using active (i.e., task) and passive (i.e., baseline) periods of equal duration and bandwidth. Such images are typically called pseudo-*t* maps, with units (pseudo-*t*) that reflect noise-normalized power differences (i.e., active vs. passive) per voxel. This generated participant-level pseudo-*t* maps for each time-frequency-specific response identified in the sensor-level permutation analysis, which was then transformed into standardized space using the transform previously applied to the structural MRI volume and spatially resampled.

Resultant pseudo-*t* maps were averaged within participants across the time windows used to image neural activity during encoding and maintenance periods, separately. The averaged source maps did not include segments representative of time windows spanning two different phases of the task (e.g., encoding and maintenance). Effects of testosterone were analyzed using whole-brain ANCOVA models in SPM12 (*141*). Testosterone (natural log-transformed), participant sex, and the interactive effect

between sex and testosterone were used as variables of interest. Participants' chronological age and time of salivary hormone collection were included in the model as variables of no interest. To account for multiple comparisons, a significance threshold of $p < .005$ was used in all statistical maps to identify significant clusters, in addition to a cluster threshold of 8 contiguous (4x4x4 mm) voxels (i.e. 512 mm^3).

Results:

Testosterone and Behavioral Results

Demographic and behavioral analyses were conducted on the 89 youth who completed the Sternberg VWM task and provided salivary testosterone samples. Average salivary testosterone measured in this sample was 33.09 pg/mL (SD = 24.96). Measures of normality indicated that testosterone values were not normally distributed (skewness = 1.89, kurtosis = 1.50), thus measurements were natural log-transformed ($M = 3.23$, $SD = 0.79$). Testosterone values were significantly correlated with age ($r = .64$, $p < .001$; Figure 12), but did not significantly differ between sexes ($t(87) = -1.26$, $p = .21$). Average accuracy on the VWM task was 83.92% ($SD = 10.44$), and accuracy was significantly positively correlated with age, such that older participants performed significantly better than younger participants on the task ($r = .59$, $p < .001$). An independent samples t-test showed that males and females did not significantly differ in accuracy ($t(87) = 0.29$, $p = .77$), however, linear regression analysis showed that females with higher testosterone had significantly higher accuracy than males, controlling for age ($\beta = 0.99$, $p = .01$; Figure 12). Average reaction time on the task was 1209.31 ms ($SD = 265.27$), and reaction time was significantly negatively correlated with age such that older participants responded significantly faster than younger participants ($r = -.65$, $p < .001$). Males and females did not significantly differ in reaction time ($t(87) = 1.48$, $p = .14$), and there were no significant effects of testosterone on reaction time, controlling for age ($\beta = 0.11$, $p = .39$).

Of the 89 participants who completed the modified Sternberg VWM task, we excluded 10 for noisy MEG data. Therefore, the final sample used for neural analyses consisted of 79 participants (*M* = 10.29 years, *SD* = 2.50; 36 females; 6 left-handed), and neither age (t(77) = -.72, *p* = .48) nor testosterone (t(77) = -1.43, *p* = .16) significantly differed by sex. To ensure that the MEG data of the final sample was not biased by development, we tested for a relationship between age and the number of trials retained for analysis. The number of trials retained was not significantly correlated with age (*r* = .15, *p* = .17) or testosterone (*r* = -.01, *p* = .96), and did not significantly differ by sex (*t*(77) = .98, *p* = .33).

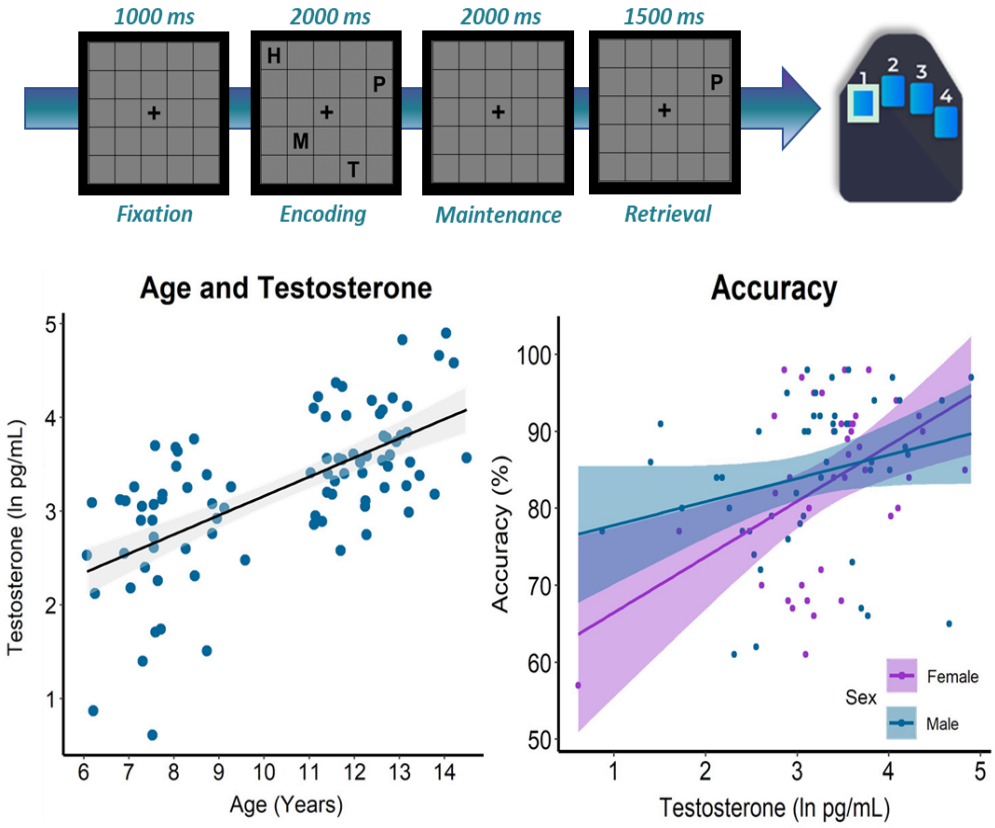

Figure 12: Modified Sternberg VWM task and behavior.

(Top) Example trial of the modified Sternberg VWM task and the corresponding correct response on the button response pad. (Bottom Left) Testosterone levels were significantly correlated with chronological age. (Bottom Right) Participants with higher levels of testosterone were significantly more accurate on the task, with this relationship being stronger among females than males.

MEG Sensor-Level and Source-Level Results

Statistical examination of sensor-level time-frequency spectrograms showed a significant increase in theta (4-7 Hz) power, relative to baseline, from 100 – 2,200 ms. From 400-4,400 ms after encoding onset there was a significant decrease in alpha (8-12 Hz) power, relative to baseline. During the maintenance period there was a strong increase in alpha (9-14 Hz), relative to baseline, from 2,550-2,900 ms, which transformed into more narrow alpha activity (8-12 Hz) from 3,100 ms to the end of the maintenance period (Figure 13; $p < 0.0001$, permutation corrected). These significant alpha and theta responses were divided into 400 ms non-overlapping time bins for source reconstruction.

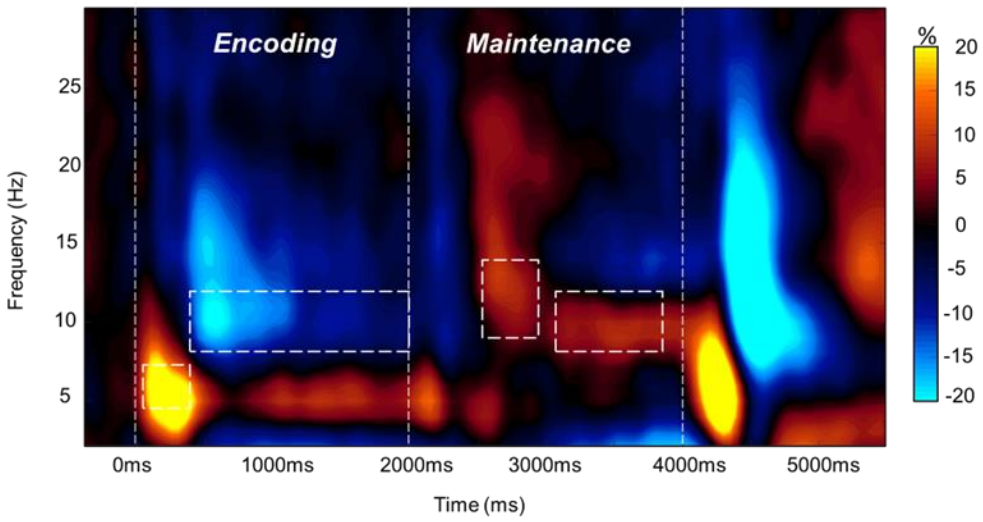

Figure 13: Grand-Averaged MEG Sensor-Level Spectrogram.

Grand-averaged time-frequency spectrogram taken from a representative sensor (MEG2043). Time is denoted on the x-axis (0.0 s = encoding onset) and frequency (Hz) is denoted on the y-axis. Time-frequency windows that were used for source estimation are denoted by the dashed white boxes. The spectrogram is shown in percent power change from baseline, with the color scale shown to the right of the spectrogram.

Specifically, we applied a beamformer to the following windows: 4-7 Hz from 100 to 500 ms, 8-12 Hz from 400 to 2,000 ms, 9-14 Hz from 2,550-2,900 ms, and 8-12 Hz from 3,100-3,900 ms.

Average beamformer images across all participants revealed that the early theta (4-7 Hz) increase from baseline was strongest in bilateral occipital cortices, while the alpha (8-12 Hz) decrease response during encoding began in bilateral occipital regions and

extended anteriorly to include left temporal regions as encoding progressed. During maintenance, increases in alpha (9-14 Hz), relative to baseline, were weakly seen in right inferior-occipital cortices. Alpha (8-12 Hz) increases from baseline were strongest in the right posterior occipital cortices.

Sexually-Divergent Effects of Testosterone in Oscillatory Power

Testosterone-by-sex interaction effects on theta (4-7 Hz) activity during encoding were found in the right cerebellar cortex ($F(1,66) = 11.79$, $p = .001$; Figure 14). Females with greater testosterone exhibited significantly weaker theta increases from baseline, while males exhibited the opposite relationship. Interactive effects on alpha (8-12 Hz) activity were found in the left middle temporal gyrus ($F(1,73) = 10.58$, $p = .002$; Figure 14). Females with higher testosterone levels showed stronger alpha decreases from baseline than those with lower testosterone, with males showing the opposite pattern. There were no significant sex-by-testosterone effects found during the maintenance period. All significant sex-by-testosterone effects controlled for the main effects of sex, testosterone, age, and time of salivary testosterone collection.

Main Effects of Endogenous Testosterone on Neural Oscillatory Responses

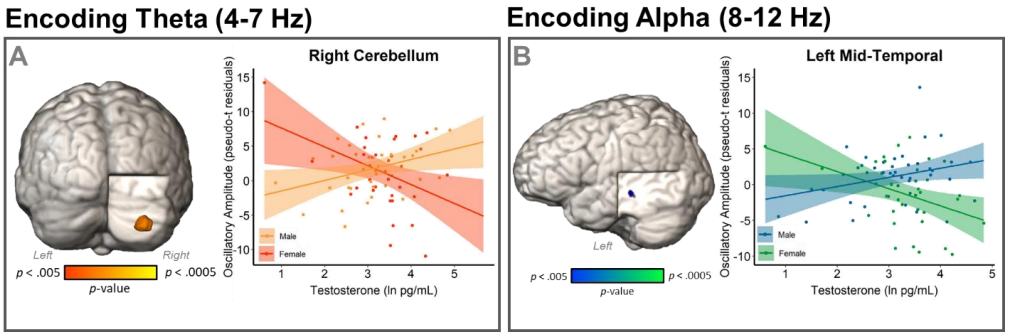

Figure 14: Sexually divergent effects of testosterone on neural oscillations serving working memory encoding.

Whole-brain ANCOVA maps and associated scatterplots showing the interactive effect at the peak voxel, with natural-log testosterone value (pg/mL) on the x-axes and residuals of the oscillatory amplitude in pseudo-t units on the y-axes, controlling for age and collection time. (A) Females with higher testosterone levels had weaker theta increases from baseline than females with lower testosterone levels, with males showing the opposite effect. (B) Females with higher testosterone levels had stronger alpha decreases from baseline than females with lower testosterone levels. The opposite was true for males.

Whole-brain, voxel-wise ANCOVA results revealed significant main effects of testosterone on alpha oscillatory activity (9-14 Hz) in right parahippocampal gyrus ($F(1,68) = 14.96$, $p < .001$; Figure 15) and right cerebellum ($F(1,68) = 9.05$, $p = .004$; Figure 15), suggesting that participants with greater levels of testosterone had weaker alpha decreases from baseline in these regions during early maintenance. During the latter portion of maintenance, effects of testosterone on alpha oscillatory activity (8-12 Hz) were significant in the left inferior parietal ($F(1,61) = 10.31$, $p = .002$; Figure 4) and left occipital cortices ($F(1,61) = 11.75$, $p = .001$; Figure 15), indicating that in these two regions participants with higher testosterone levels had weaker decreases in alpha activity. All effects controlled for the effects of chronological age, sex, and time of salivary testosterone collection.

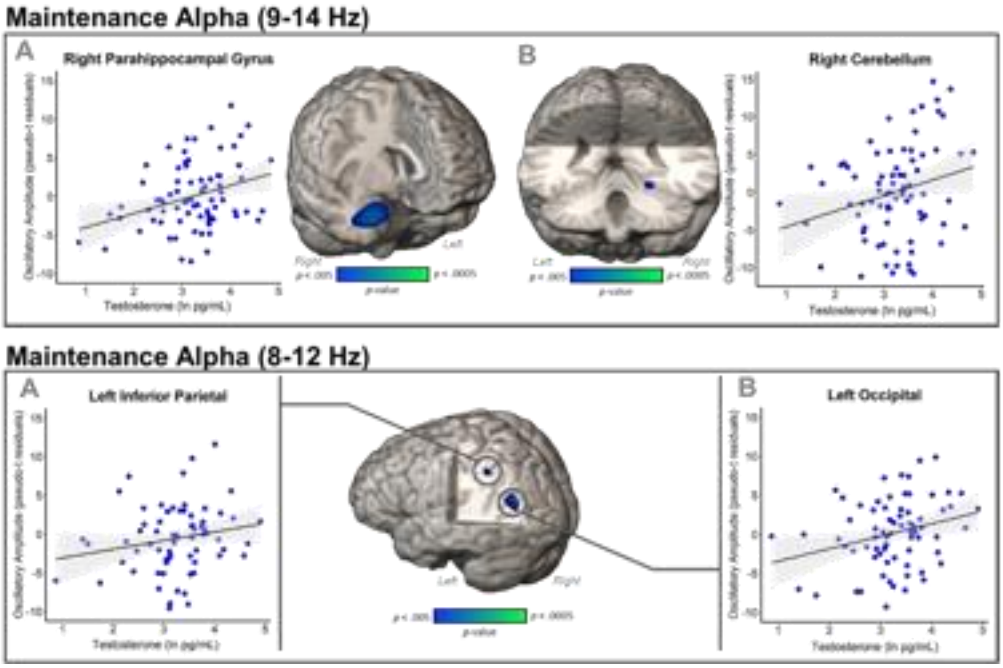

Figure 15: Effects of testosterone on the neural oscillations serving working memory maintenance.

Whole-brain ANCOVA maps and associated scatterplots showing the relationship at the peak voxel, with natural log of testosterone (pg/mL) on the x-axes and oscillatory amplitude in residuals of pseudo-t units on the y-axes. (A-C) Alpha oscillations became stronger with increasing age in the right occipital cortices, right parietal, left prefrontal, and left occipito-temporal cortices.

Discussion:

In this cross-sectional sample of 6-14-year-old youth, we examined how endogenous testosterone levels were related to the neural oscillatory underpinnings of VWM, above and beyond the effects of chronological age. These results are the first to provide data showing the relationship between endogenous testosterone and neural oscillations serving the encoding and maintenance phases of VWM in a sample of typically-developing youth. As expected, testosterone and chronological age were tightly coupled, such that older youth had higher testosterone levels. Behaviorally, females with higher endogenous testosterone performed better on the task than those with lower testosterone. At the neural level, testosterone's effects on oscillatory activity during encoding significantly differed between males and females. Females with higher testosterone levels exhibited a weaker

theta increase from baseline in the right cerebellar cortex during the 100-500 ms period after encoding onset, whereas males exhibited the opposite pattern. Conversely, females with higher testosterone also had significantly stronger alpha oscillations (i.e., decreases from baseline) in the left temporal cortex during the 400-2000 ms period after encoding onset, with males again exhibiting the opposite relationship between testosterone and oscillatory activity. For both of the maintenance responses (9-14 and 8-12 Hz), participants with lower testosterone exhibited stronger oscillations (i.e., decreases from baseline) than those with higher testosterone. Our results suggest that testosterone's effects on network maturation may be distinguishable from those of chronological age.

Research in healthy adults suggests sex differences in VWM performance that depend upon the experimental paradigm or neuropsychological test used (*142, 143*). However, developmental sex differences in VWM performance are inconsistently reported (*21, 144, 145*), with no strong agreement on whether sex differences emerge in childhood during language acquisition, or adolescence when cortical networks are being refined (*144*). Much of this discrepancy is attributable to differences in the neuropsychological test used to measure VWM (e.g., Complex Span, CVLT (California Verbal Learning Test), or COWAT (Controlled Oral Word Association Test)), with slightly different domains of working memory being targeted by each measure (i.e., tests of verbal fluency measuring vocabulary and semantic memory or word list tests measuring episodic recall). Our showing a positive relationship between VWM accuracy and testosterone in females suggests that incorporating pubertal hormones in analyses may be useful for identifying the emergence of sex differences in VWM performance.

Interestingly, during encoding there were only interactive effects of sex and testosterone, with higher testosterone females having weaker theta increases in the right cerebellar cortices and stronger alpha decreases in the left middle temporal gyrus.

Cerebellar oscillatory activity has been implicated in working memory (*31, 45, 46*), with theta oscillations reflecting cerebellar communication within visuomotor adaptation networks (*146*), and serial ordering of stimuli for spatial memory (*147*). On the other hand, regions of the left temporal cortex critically support language processing, and sustained alpha decreases in left temporal and inferior frontal cortices have been associated with sub-vocal rehearsal during encoding and maintenance (*30, 32, 43, 79, 120*). Sex differences during encoding have been previously reported in youth, with older females exhibiting stronger inferior frontal alpha activity than males (*32*). Researchers suggested that this indicated differential maturational trends, whereby cortical regions supporting VWM mature at different times in males and females. In the context of our findings, females with higher testosterone may rely less upon spatial strategies for successful stimulus encoding and more upon sub-vocal rehearsal. Alternatively, testosterone may contribute to network refinement in females by weakening theta activity in this cerebellar region to be more strongly utilized in other areas.

Our alpha findings show significant effects of testosterone in left-lateralized language regions only during encoding and late maintenance. In contrast, during early maintenance, we found testosterone effects in the right parahippocampus and right cerebellum, outside of the 8-12 Hz frequency range. The parahippocampal gyrus has been shown to facilitate contextual associations for stronger stimulus encoding (*148-151*) and serve as a short-term memory buffer with increasing memory load (*152*). Sustained decreases in alpha activity within the inferior parietal and occipital cortices, along with portions of the left temporal cortex, have been suggested by previous VWM investigations to facilitate active maintenance of verbal stimuli through the phonological loop (*31, 65*). However, we see that during maintenance, greater testosterone is associated with weaker decreases in alpha (i.e., weaker oscillations) in these left inferior parietal and occipital cortices, as well

as right hippocampal and cerebellar cortices. If testosterone aids in fine-tuning developmental networks, participants with greater hormones may rely on these specific nodes less than their low testosterone counterparts as a product of increased network specialization. Future research using a longitudinal design should probe associations between testosterone and functional connectivity within VWM networks, to better delineate how individual testosterone levels interact with the maturation of VWM.

Before closing, we must acknowledge the limitations of our investigation and offer suggestions for future work. Primarily, with a cross-sectional sample it is difficult to predict how testosterone levels will change in each individual over time. Future studies should utilize a longitudinal design, to capture how the timing and tempo of puberty may affect testosterone levels, and in turn, affect the neural oscillatory underpinnings of VWM. Salivary hormone collection has proven to be an effective method of analyzing hormonal effects on neural function, but it can be challenging to ensure that collection is done at the same time of day for each participant to account for the cyclical nature of testosterone levels. While testosterone's diurnal cycle is far less than other hormones, like cortisol, we still used collection time as a covariate of no interest in this study. Nevertheless, future work can greatly benefit from collecting hair samples, to provide an average estimate of hormone levels over a longer period (*153*). Lastly, future investigations would benefit from larger sample sizes providing more power to account for variables like race, SES, and body mass index (BMI) which are known to affect hormone levels and puberty onset (*154*). Additionally, this can allow researchers to examine how factors like trauma experiences or mental health symptomology might moderate the relationship between oscillatory activity and testosterone levels.

The data presented herein was the first to show testosterone's effects, above and beyond the effects of age, on encoding and maintenance-related oscillatory activity, in a

typically developing sample of youth and children. There were significant effects of testosterone on task accuracy and alpha and theta activity during encoding that significantly differed by sex, and main effects of testosterone on oscillatory activity in key working memory-related cortices during maintenance. These results shed light on testosterone's region and sex-specific effects and offer evidence for its role in fine-tuning developmental processes.

CONCLUSIONS

The strength of these studies lies in evidence that age and testosterone are uniquely related to oscillatory activity in developing youth, in a manner suggesting that, despite chronological age and endogenous testosterone levels being tightly coupled, age-related developmental trajectories may be significantly different from developmental modifications that occur in response to changes in pubertal hormones. Furthermore, this work suggests that within a working memory network, developmentally sensitive regions have functional connectivity that dynamically change with age in a behaviorally relevant manner. Given the relative dearth of literature quantifying the effects of endogenous testosterone on cortical activity serving executive functions from childhood to adolescence, this work offers a link between animal studies and behavioral investigations.

Broadly speaking, the language system is one of the predominant systems supporting VWM encoding during childhood and adolescence. During encoding and maintenance, oscillatory activity differences between older and younger youth were consistently found within regions supporting phonological encoding (i.e., left occipital-temporal and inferior parietal cortices) and bilateral frontal cortices. Even individual differences in testosterone levels revealed that among females, the mid-temporal cortex significantly varied in the encoding-related activity with testosterone, in addition to the inferior parietal and occipital cortices for maintenance-related activity across sexes. In alignment with previous work in developing samples, maturation of the network calls upon distributed regions, with the right angular gyrus being recruited in a supportive role during maintenance. Verbal working memory is heavily associated with language and reading acquisition, but these studies show that the language network's role in VWM processing is still developing, regarding oscillatory power and functional connectivity.

Within the alpha band, these reports show that frontal and parietal cortices supporting the use of spatial attention to carry out encoding and maintenance are also under development. The Sternberg VWM task requires a level of visual and spatial processing. With oscillatory activity in parietal and occipital cortices changing with development, our data provides insight into the possibility that differential maturational trends could be occurring concerning age and testosterone. Based on previous work showing age-related decreases in grey matter thickness in higher association cortices and modified dendrite morphology on pyramidal neurons as a function of testosterone concentration, it logically follows that different patterns of oscillatory power would emerge between youth during childhood and adolescence. These results also provide evidence for long-range functional connectivity reflecting the distributed nature of this working memory network.

Other than alpha results, findings within the theta band are mostly centered on the visual system and the cerebellum, pointing to the ubiquitous nature of the cerebellum in higher-order processing, and the continuous development of information transfer in the visual system during adolescence. Given the amount of previous WM studies that have reported findings of frontal theta activity, and the frontal cortex's protracted development, it is interesting that most results in the theta band were found in posterior cortices. Future studies are needed to demystify the role of posterior theta oscillatory activity during development, especially given the plethora of studies focused on frontal theta activity during working memory processes.

This pattern of findings reveals that during development, there are dynamic changes in language and attentional systems that lead to massive gains in VWM capacity. The connectivity analyses provide strong support for the notion that during development there is coordination between phonological and visual attention systems to successfully engage in VWM. This has huge implications for knowledge of VWM development in typically

developing children, because it can inform educators, physicians, clinicians, and scientists about the neural regions and neural systems that experience the most change during childhood and development.

These three studies can help advance the field of developmental neuroscience, by exhibiting the utility of endogenous testosterone in examining developmental patterns of change. However, these analyses have also further localized the regions in a distributed VWM network that are sensitive to the typical development of youth and explained how communication between these sensitive regions would also scale with age. Overall, this body of work demonstrates that age and testosterone affect different regions of the phonological system during encoding, with influence over some regions of the visual and selective-attention systems. During maintenance, some of these same age-sensitive regions are recruited to aid in top-down control processes, with less utilization of attention and phonological processing with age.

BIBLIOGRAPHY

1. S.-J. Blakemore, S. Choudhury, Development of the adolescent brain: implications for executive function and social cognition. *Journal of Child Psychology and Psychiatry* **47**, 296-312 (2006).
2. N. Gogtay *et al.*, Dynamic mapping of human cortical development during childhood through early adulthood. *Proceedings of the National Academy of Sciences* **101**, 8174-8179 (2004).
3. D. Fuhrmann, L. J. Knoll, S.-J. Blakemore, Adolescence as a Sensitive Period of Brain Development. *Trends in Cognitive Sciences* **19**, 558-566 (2015).
4. B. Larsen, B. Luna, Adolescence as a neurobiological critical period for the development of higher-order cognition. *Neuroscience & Biobehavioral Reviews* **94**, 179-195 (2018).
5. M. L. Byrne *et al.*, A systematic review of adrenarche as a sensitive period in neurobiological development and mental health. *Developmental Cognitive Neuroscience* **25**, 12-28 (2017).
6. L. D. Dorn, Measuring puberty. *J Adolesc Health* **39**, 625-626 (2006).
7. T. Paus *et al.*, Sexual dimorphism in the adolescent brain: Role of testosterone and androgen receptor in global and local volumes of grey and white matter. *Hormones and Behavior* **57**, 63-75 (2010).
8. J. S. Peper *et al.*, Sex steroids and brain structure in pubertal boys and girls. *Psychoneuroendocrinology* **34**, 332-342 (2009).
9. J. E. Bramen *et al.*, Puberty influences medial temporal lobe and cortical gray matter maturation differently in boys than girls matched for sexual maturity. *Cereb Cortex* **21**, 636-646 (2011).
10. J.-R. Chen, T.-J. Wang, S.-H. Lim, Y.-J. Wang, G.-F. Tseng, Testosterone modulation of dendritic spines of somatosensory cortical pyramidal neurons. *Brain Structure and Function* **218**, 1407-1417 (2013).
11. M. Li, M. Masugi-Tokita, K. Takanami, S. Yamada, M. Kawata, Testosterone has sublayer-specific effects on dendritic spine maturation mediated by BDNF and PSD-95 in pyramidal neurons in the hippocampus CA1 area. *Brain Research* **1484**, 76-84 (2012).
12. C. Laube, W. Van Den Bos, Y. Fandakova, The relationship between pubertal hormones and brain plasticity: Implications for cognitive training in adolescence. *Developmental Cognitive Neuroscience* **42**, 100753 (2020).
13. N. Cowan, Working Memory Underpins Cognitive Development, Learning, and Education. *Educational Psychology Review* **26**, 197-223 (2014).
14. H. M. Conklin, M. Luciana, C. J. Hooper, R. S. Yarger, Working Memory Performance in Typically Developing Children and Adolescents: Behavioral Evidence of Protracted Frontal Lobe Development. *Developmental Neuropsychology* **31**, 103-128 (2007).
15. S. F. Ahmed, A. Ellis, K. P. Ward, N. Chaku, P. E. Davis-Kean, Working memory development from early childhood to adolescence using two nationally representative samples. *Developmental Psychology*, (2022).
16. T. P. Alloway, G. E. Banner, P. Smith, Working memory and cognitive styles in adolescents' attainment. *British Journal of Educational Psychology* **80**, 567-581 (2010).
17. S. E. Gathercole, S. J. Pickering, C. Knight, Z. Stegmann, Working memory skills and educational attainment: evidence from national curriculum assessments at 7 and 14 years of age. *Applied Cognitive Psychology* **18**, 1-16 (2004).
18. C. Huang-Pollock, Z. Shapiro, H. Galloway-Long, A. Weigard, Is Poor Working Memory a Transdiagnostic Risk Factor for Psychopathology? *Journal of Abnormal Child Psychology* **45**, 1477-1490 (2017).

19. M. T. Banich *et al.*, Cognitive control mechanisms, emotion and memory: A neural perspective with implications for psychopathology. *Neuroscience & Biobehavioral Reviews* **33**, 613-630 (2009).
20. A. Baddeley, Working Memory: Theories, Models, and Controversies. *Annual Review of Psychology* **63**, 1-29 (2012).
21. S. E. Gathercole, S. J. Pickering, B. Ambridge, H. Wearing, The structure of working memory from 4 to 15 years of age. *Dev Psychol* **40**, 177-190 (2004).
22. J. Andre, M. Picchioni, R. Zhang, T. Toulopoulou, Working memory circuit as a function of increasing age in healthy adolescence: A systematic review and meta-analyses. *Neuroimage Clin* **12**, 940-948 (2016).
23. E. D. O'Hare, L. H. Lu, S. M. Houston, S. Y. Bookheimer, E. R. Sowell, Neurodevelopmental changes in verbal working memory load-dependency: An fMRI investigation. *NeuroImage* **42**, 1678-1685 (2008).
24. V. M. Vogan, B. R. Morgan, T. L. Powell, M. L. Smith, M. J. Taylor, The neurodevelopmental differences of increasing verbal working memory demand in children and adults. *Developmental Cognitive Neuroscience* **17**, 19-27 (2016).
25. M. E. Thomason *et al.*, Development of Spatial and Verbal Working Memory Capacity in the Human Brain. *Journal of Cognitive Neuroscience* **21**, 316-332 (2009).
26. W. Singer, Neuronal oscillations: unavoidable and useful? *European Journal of Neuroscience* **48**, 2389-2398 (2018).
27. G. Buzsáki, A. Draguhn, Neuronal oscillations in cortical networks. *Science* **304**, 1926-1929 (2004).
28. O. Jensen, C. D. Tesche, Frontal theta activity in humans increases with memory load in a working memory task. *European Journal of Neuroscience* **15**, 1395-1399 (2002).
29. A. L. Proskovec, E. Heinrichs-Graham, T. W. Wilson, Load modulates the alpha and beta oscillatory dynamics serving verbal working memory. *NeuroImage* **184**, 256-265 (2019).
30. A. L. Proskovec, A. I. Wiesman, E. Heinrichs-Graham, T. W. Wilson, Load effects on spatial working memory performance are linked to distributed alpha and beta oscillations. *Human Brain Mapping* **40**, 3682-3689 (2019).
31. E. Heinrichs-Graham, T. W. Wilson, Spatiotemporal oscillatory dynamics during the encoding and maintenance phases of a visual working memory task. *Cortex* **69**, 121-130 (2015).
32. C. M. Embury *et al.*, Neural dynamics of verbal working memory processing in children and adolescents. *NeuroImage* **185**, 191-197 (2019).
33. E. Heinrichs-Graham, E. A. Walker, J. A. Eastman, M. R. Frenzel, R. W. McCreery, Amount of Hearing Aid Use Impacts Neural Oscillatory Dynamics Underlying Verbal Working Memory Processing for Children With Hearing Loss. *Ear Hear* **43**, 408-419 (2022).
34. E. Heinrichs-Graham *et al.*, The impact of mild-to-severe hearing loss on the neural dynamics serving verbal working memory processing in children. *Neuroimage Clin* **30**, 102647 (2021).
35. K. S. Scherf, J. A. Sweeney, B. Luna, Brain basis of developmental change in visuospatial working memory. *J Cogn Neurosci* **18**, 1045-1058 (2006).
36. M. D. Rosenberg *et al.*, Behavioral and Neural Signatures of Working Memory in Childhood. *J Neurosci* **40**, 5090-5104 (2020).
37. H. Kwon, A. L. Reiss, V. Menon, Neural basis of protracted developmental changes in visuo-spatial working memory. *Proc Natl Acad Sci U S A* **99**, 13336-13341 (2002).
38. N. Ramnani, A. M. Owen, Anterior prefrontal cortex: insights into function from anatomy and neuroimaging. *Nat Rev Neurosci* **5**, 184-194 (2004).

39. S. M. Ravizza, M. R. Delgado, J. M. Chein, J. T. Becker, J. A. Fiez, Functional dissociations within the inferior parietal cortex in verbal working memory. *Neuroimage* **22**, 562-573 (2004).
40. Y. Østby, C. K. Tamnes, A. M. Fjell, K. B. Walhovd, Morphometry and connectivity of the fronto-parietal verbal working memory network in development. *Neuropsychologia* **49**, 3854-3862 (2011).
41. L. Attout, L. Ordonez Magro, A. Szmalec, S. Majerus, The developmental neural substrates of item and serial order components of verbal working memory. *Hum Brain Mapp* **40**, 1541-1553 (2019).
42. C. Rottschy *et al.*, Modelling neural correlates of working memory: A coordinate-based meta-analysis. *NeuroImage* **60**, 830-846 (2012).
43. C. M. Embury *et al.*, Altered Brain Dynamics in Patients With Type 1 Diabetes During Working Memory Processing. *Diabetes* **67**, 1140-1148 (2018).
44. T. J. McDermott *et al.*, Male veterans with PTSD exhibit aberrant neural dynamics during working memory processing: an MEG study. *Journal of Psychiatry & Neuroscience* **41**, 251-260 (2016).
45. A. L. Proskovec, E. Heinrichs-Graham, T. W. Wilson, Aging modulates the oscillatory dynamics underlying successful working memory encoding and maintenance. *Human Brain Mapping* **37**, 2348-2361 (2016).
46. T. W. Wilson *et al.*, Aberrant Neuronal Dynamics during Working Memory Operations in the Aging HIV-Infected Brain. *Sci Rep* **7**, 41568 (2017).
47. A. I. Wiesman *et al.*, Quiet connections: Reduced fronto-temporal connectivity in nondemented Parkinson's Disease during working memory encoding. *Hum Brain Mapp* **37**, 3224-3235 (2016).
48. W. Klimesch, EEG alpha and theta oscillations reflect cognitive and memory performance: a review and analysis. *Brain Research Reviews* **29**, 169-195 (1999).
49. J. F. Cavanagh, M. J. Frank, Frontal theta as a mechanism for cognitive control. *Trends in Cognitive Sciences* **18**, 414-421 (2014).
50. J. Fellrath, A. Mottaz, A. Schnider, A. G. Guggisberg, R. Ptak, Theta-band functional connectivity in the dorsal fronto-parietal network predicts goal-directed attention. *Neuropsychologia* **92**, 20-30 (2016).
51. A. D. Killanin *et al.*, Trauma moderates the development of the oscillatory dynamics serving working memory in a sex-specific manner. *Cerebral Cortex*, (2022).
52. A. L. Proskovec, A. I. Wiesman, E. Heinrichs-Graham, T. W. Wilson, Load effects on spatial working memory performance are linked to distributed alpha and beta oscillations. *Hum Brain Mapp* **40**, 3682-3689 (2019).
53. A. L. Proskovec, A. I. Wiesman, E. Heinrichs-Graham, T. W. Wilson, Beta Oscillatory Dynamics in the Prefrontal and Superior Temporal Cortices Predict Spatial Working Memory Performance. *Scientific Reports* **8**, (2018).
54. S. Taulu, J. Simola, Spatiotemporal signal space separation method for rejecting nearby interference in MEG measurements. *Phys Med Biol* **51**, 1759-1768 (2006).
55. S. Taulu, J. Simola, M. Kajola, Applications of the signal space separation method. *IEEE Transactions on Signal Processing* **53**, 3359-3372 (2005).
56. A. I. Wiesman, T. W. Wilson, Attention modulates the gating of primary somatosensory oscillations. *Neuroimage* **211**, 116610 (2020).
57. M. A. Uusitalo, R. J. Ilmoniemi, Signal-space projection method for separating MEG or EEG into components. *Medical & Biological Engineering & Computing* **35**, 135-140 (1997).

58. N. Papp, P. Ktonas, Critical evaluation of complex demodulation techniques for the quantification of bioelectrical activity. *Biomed Sci Instrum* **13**, 135-145 (1977).
59. C. K. Kovach, P. E. Gander, The demodulated band transform. *Journal of Neuroscience Methods* **261**, 135-154 (2016).
60. M. D. Ernst, Permutation Methods: A Basis for Exact Inference. *Statistical Science* **19**, 676-685 (2004).
61. E. Maris, R. Oostenveld, Nonparametric statistical testing of EEG- and MEG-data. *Journal of Neuroscience Methods* **164**, 177-190 (2007).
62. J. Gross *et al.*, Dynamic imaging of coherent sources: Studying neural interactions in the human brain. *Proceedings of the National Academy of Sciences* **98**, 694-699 (2001).
63. A. Hillebrand, K. D. Singh, I. E. Holliday, P. L. Furlong, G. R. Barnes, A new approach to neuroimaging with magnetoencephalography. *Human Brain Mapping* **25**, 199-211 (2005).
64. A. Baddeley, Working memory. *Science* **255**, 556-559 (1992).
65. C. J. Price, A review and synthesis of the first 20 years of PET and fMRI studies of heard speech, spoken language and reading. *Neuroimage* **62**, 816-847 (2012).
66. T. W. Wilson, A. C. Leuthold, S. M. Lewis, A. P. Georgopoulos, P. J. Pardo, Cognitive dimensions of orthographic stimuli affect occipitotemporal dynamics. *Exp Brain Res* **167**, 141-147 (2005).
67. T. W. Wilson, A. C. Leuthold, S. M. Lewis, A. P. Georgopoulos, P. J. Pardo, The time and space of lexicality: a neuromagnetic view. *Exp Brain Res* **162**, 1-13 (2005).
68. T. W. Wilson *et al.*, Reading in a deep orthography: neuromagnetic evidence for dual-mechanisms. *Exp Brain Res* **180**, 247-262 (2007).
69. S. Dehaene, L. Cohen, The unique role of the visual word form area in reading. *Trends Cogn Sci* **15**, 254-262 (2011).
70. S. V. Di Pietro, Karipidis, II, G. Pleisch, S. Brem, Neurodevelopmental trajectories of letter and speech sound processing from preschool to the end of elementary school. *Dev Cogn Neurosci* **61**, 101255 (2023).
71. L. Dugué, R. VanRullen, Transcranial Magnetic Stimulation Reveals Intrinsic Perceptual and Attentional Rhythms. *Front Neurosci* **11**, 154 (2017).
72. S. D. Muthukumaraswamy, K. D. Singh, J. B. Swettenham, D. K. Jones, Visual gamma oscillations and evoked responses: variability, repeatability and structural MRI correlates. *Neuroimage* **49**, 3349-3357 (2010).
73. A. I. Wiesman, E. Heinrichs-Graham, A. L. Proskovec, T. J. McDermott, T. W. Wilson, Oscillations during observations: Dynamic oscillatory networks serving visuospatial attention. *Human Brain Mapping* **38**, 5128-5140 (2017).
74. A. I. Wiesman *et al.*, Aberrant occipital dynamics differentiate HIV-infected patients with and without cognitive impairment. *Brain* **141**, 1678-1690 (2018).
75. A. I. Wiesman, T. W. Wilson, The impact of age and sex on the oscillatory dynamics of visuospatial processing. *NeuroImage* **185**, 513-520 (2019).
76. A. D. Killanin *et al.*, Development and sex modulate visuospatial oscillatory dynamics in typically-developing children and adolescents. *NeuroImage* **221**, 117192 (2020).
77. J. M. Abel, D. M. Witt, E. F. Rissman, Sex differences in the cerebellum and frontal cortex: roles of estrogen receptor alpha and sex chromosome genes. *Neuroendocrinology* **93**, 230-240 (2011).
78. J. E. Desmond, J. D. Gabrieli, A. D. Wagner, B. L. Ginier, G. H. Glover, Lobular patterns of cerebellar activation in verbal working-memory and finger-tapping tasks as revealed by functional MRI. *J Neurosci* **17**, 9675-9685 (1997).

79. E. Heinrichs-Graham, T. W. Wilson, Spatiotemporal oscillatory dynamics during the encoding and maintenance phases of a visual working memory task. *Cortex* **69**, 121-130 (2015).
80. M. Bonnefond, O. Jensen, Alpha Oscillations Serve to Protect Working Memory Maintenance against Anticipated Distracters. *Current Biology* **22**, 1969-1974 (2012).
81. B. F. Händel, T. Haarmeier, O. Jensen, Alpha Oscillations Correlate with the Successful Inhibition of Unattended Stimuli. *Journal of Cognitive Neuroscience* **23**, 2494-2502 (2011).
82. O. Jensen, Oscillations in the Alpha Band (9-12 Hz) Increase with Memory Load during Retention in a Short-term Memory Task. *Cerebral Cortex* **12**, 877-882 (2002).
83. M. D'Esposito, B. R. Postle, The Cognitive Neuroscience of Working Memory. *Annual Review of Psychology* **66**, 115-142 (2015).
84. T. B. Christophel, P. C. Klink, B. Spitzer, P. R. Roelfsema, J.-D. Haynes, The Distributed Nature of Working Memory. *Trends in Cognitive Sciences* **21**, 111-124 (2017).
85. A. H. Lara, J. D. Wallis, The Role of Prefrontal Cortex in Working Memory: A Mini Review. *Frontiers in Systems Neuroscience* **9**, (2015).
86. D. A. Crowe *et al.*, Prefrontal neurons transmit signals to parietal neurons that reflect executive control of cognition. *Nature Neuroscience* **16**, 1484-1491 (2013).
87. C. E. Curtis, M. D'Esposito, Persistent activity in the prefrontal cortex during working memory. *Trends Cogn Sci* **7**, 415-423 (2003).
88. E. F. Ester, T. C. Sprague, J. T. Serences, Parietal and Frontal Cortex Encode Stimulus-Specific Mnemonic Representations during Visual Working Memory. *Neuron* **87**, 893-905 (2015).
89. A. H. Lara, J. D. Wallis, Executive control processes underlying multi-item working memory. *Nature Neuroscience* **17**, 876-883 (2014).
90. E. K. Miller, J. D. Cohen, An Integrative Theory of Prefrontal Cortex Function. *Annual Review of Neuroscience* **24**, 167-202 (2001).
91. S. B. Brahmbhatt, T. McAuley, D. M. Barch, Functional developmental similarities and differences in the neural correlates of verbal and nonverbal working memory tasks. *Neuropsychologia* **46**, 1020-1031 (2008).
92. C. Rothmayr *et al.*, Dissociation of neural correlates of verbal and non-verbal visual working memory with different delays. *Behavioral and Brain Functions* **3**, 56 (2007).
93. S. K. Swaminathan, D. J. Freedman, Preferential encoding of visual categories in parietal cortex compared with prefrontal cortex. *Nature Neuroscience* **15**, 315-320 (2012).
94. C. Lebel, L. Walker, A. Leemans, L. Phillips, C. Beaulieu, Microstructural maturation of the human brain from childhood to adulthood. *NeuroImage* **40**, 1044-1055 (2008).
95. T. J. Eluvathingal, K. M. Hasan, L. Kramer, J. M. Fletcher, L. Ewing-Cobbs, Quantitative Diffusion Tensor Tractography of Association and Projection Fibers in Normally Developing Children and Adolescents. *Cerebral Cortex* **17**, 2760-2768 (2007).
96. V. Menon, Developmental pathways to functional brain networks: emerging principles. *Trends Cogn Sci* **17**, 627-640 (2013).
97. Q. J. Yap *et al.*, Tracking cerebral white matter changes across the lifespan: insights from diffusion tensor imaging studies. *Journal of Neural Transmission* **120**, 1369-1395 (2013).
98. S. B. Brahmbhatt, D. A. White, D. M. Barch, Developmental differences in sustained and transient activity underlying working memory. *Brain Research* **1354**, 140-151 (2010).
99. E. A. Crone, C. Wendelken, S. Donohue, L. Van Leijenhorst, S. A. Bunge, Neurocognitive development of the ability to manipulate information in working memory. *Proceedings of the National Academy of Sciences* **103**, 9315-9320 (2006).

100. B. J. Nagel, M. M. Herting, E. C. Maxwell, R. Bruno, D. Fair, Hemispheric lateralization of verbal and spatial working memory during adolescence. *Brain and Cognition* **82**, 58-68 (2013).
101. P. Fries, Rhythms for Cognition: Communication through Coherence. *Neuron* **88**, 220-235 (2015).
102. K. Supekar *et al.*, Development of functional and structural connectivity within the default mode network in young children. *NeuroImage* **52**, 290-301 (2010).
103. S. Palva, S. Monto, J. M. Palva, Graph properties of synchronized cortical networks during visual working memory maintenance. *NeuroImage* **49**, 3257-3268 (2010).
104. N. M. Petro *et al.*, Eyes-closed versus eyes-open differences in spontaneous neural dynamics during development. *Neuroimage* **258**, 119337 (2022).
105. A. S. Finn, M. A. Sheridan, C. L. H. Kam, S. Hinshaw, M. D'Esposito, Longitudinal Evidence for Functional Specialization of the Neural Circuit Supporting Working Memory in the Human Brain. *Journal of Neuroscience* **30**, 11062-11067 (2010).
106. G. E. van den Bosch *et al.*, Brain connectivity during verbal working memory in children and adolescents. *Human brain mapping* **35**, 698-711 (2014).
107. J. Sato *et al.*, Alpha keeps it together: Alpha oscillatory synchrony underlies working memory maintenance in young children. *Developmental Cognitive Neuroscience* **34**, 114-123 (2018).
108. J.-P. Lachaux, E. Rodriguez, J. Martinerie, F. J. Varela, Measuring phase synchrony in brain signals. *Human Brain Mapping* **8**, 194-208 (1999).
109. T. P. Zanto, A. Gazzaley, Neural Suppression of Irrelevant Information Underlies Optimal Working Memory Performance. *The Journal of Neuroscience* **29**, 3059-3066 (2009).
110. E. K. Vogel, A. W. McCollough, M. G. Machizawa, Neural measures reveal individual differences in controlling access to working memory. *Nature* **438**, 500-503 (2005).
111. G. Lerma-Usabiaga, M. Carreiras, P. M. Paz-Alonso, Converging evidence for functional and structural segregation within the left ventral occipitotemporal cortex in reading. *Proceedings of the National Academy of Sciences* **115**, E9981-E9990 (2018).
112. M. Behrmann, D. C. Plaut, Distributed circuits, not circumscribed centers, mediate visual recognition. *Trends Cogn Sci* **17**, 210-219 (2013).
113. G. Xue, R. A. Poldrack, The Neural Substrates of Visual Perceptual Learning of Words: Implications for the Visual Word Form Area Hypothesis. *Journal of Cognitive Neuroscience* **19**, 1643-1655 (2007).
114. L. Chen *et al.*, The visual word form area (VWFA) is part of both language and attention circuitry. *Nature Communications* **10**, 5601 (2019).
115. W. Klimesch, Alpha-band oscillations, attention, and controlled access to stored information. *Trends in Cognitive Sciences* **16**, 606-617 (2012).
116. E. Wianda, B. Ross, The roles of alpha oscillation in working memory retention. *Brain and Behavior* **9**, e01263 (2019).
117. A. I. Wiesman, B. R. Groff, T. W. Wilson, Frontoparietal Networks Mediate the Behavioral Impact of Alpha Inhibition in Visual Cortex. *Cerebral Cortex* **29**, 3505-3513 (2019).
118. A. Fitch, H. Smith, S. B. Guillory, Z. Kaldy, Off to a Good Start: The Early Development of the Neural Substrates Underlying Visual Working Memory. *Front Syst Neurosci* **10**, 68 (2016).
119. E. Isbell, K. Fukuda, H. J. Neville, E. K. Vogel, Visual working memory continues to develop through adolescence. *Frontiers in Psychology* **6**, (2015).
120. M. Emch, C. C. von Bastian, K. Koch, Neural Correlates of Verbal Working Memory: An fMRI Meta-Analysis. *Frontiers in Human Neuroscience* **13**, (2019).

121. D. F. Montez, F. J. Calabro, B. Luna, Working memory improves developmentally as neural processes stabilize. *PLOS ONE* **14**, e0213010 (2019).
122. A. Arjona, B. Y. Angulo-Ruiz, E. I. Rodríguez-Martínez, C. Cabello-Navarro, C. M. Gómez, Time-frequency neural dynamics of ADHD children and adolescents during a Working Memory task. *Neuroscience Letters* **798**, 137100 (2023).
123. B. M. S. Inguscio *et al.*, Neurophysiological Verbal Working Memory Patterns in Children: Searching for a Benchmark of Modality Differences in Audio/Video Stimuli Processing. *Computational Intelligence and Neuroscience* **2021**, 1-17 (2021).
124. H. Kwon, A. L. Reiss, V. Menon, Neural basis of protracted developmental changes in visuo-spatial working memory. *Proceedings of the National Academy of Sciences* **99**, 13336-13341 (2002).
125. M. Luciana, H. M. Conklin, C. J. Hooper, R. S. Yarger, The Development of Nonverbal Working Memory and Executive Control Processes in Adolescents. *Child Development* **76**, 697-712 (2005).
126. A. D. Schweinsburg, B. J. Nagel, S. F. Tapert, fMRI reveals alteration of spatial working memory networks across adolescence. *Journal of the International Neuropsychological Society* **11**, (2005).
127. A. D. Killanin *et al.*, Trauma moderates the development of the oscillatory dynamics serving working memory in a sex-specific manner. *Cereb Cortex*, (2022).
128. L. D. Dorn, F. M. Biro, Puberty and Its Measurement: A Decade in Review. *Journal of Research on Adolescence* **21**, 180-195 (2011).
129. S.-J. Blakemore, S. Burnett, R. E. Dahl, The role of puberty in the developing adolescent brain. *Human Brain Mapping* **31**, 926-933 (2010).
130. R. L. Cunningham, B. J. Claiborne, M. Y. McGinnis, Pubertal exposure to anabolic androgenic steroids increases spine densities on neurons in the limbic system of male rats. *Neuroscience* **150**, 609-615 (2007).
131. H. Chen *et al.*, Effects of membrane androgen receptor binding on synaptic plasticity in primary hippocampal neurons. *Mol Cell Endocrinol* **554**, 111711 (2022).
132. S. J. Muthu *et al.*, Testosterone Influence on Microtubule-Associated Proteins and Spine Density in Hippocampus: Implications on Learning and Memory. *Dev Neurosci* **44**, 498-507 (2022).
133. L. Fester, G. M. Rune, Sex neurosteroids: Hormones made by the brain for the brain. *Neurosci Lett* **753**, 135849 (2021).
134. J. Dai, K. S. Scherf, Puberty and functional brain development in humans: Convergence in findings? *Developmental Cognitive Neuroscience* **39**, 100690 (2019).
135. J. E. Bramen *et al.*, Sex Matters during Adolescence: Testosterone-Related Cortical Thickness Maturation Differs between Boys and Girls. *PLoS ONE* **7**, e33850 (2012).
136. P. C. M. P. Koolschijn, J. S. Peper, E. A. Crone, The Influence of Sex Steroids on Structural Brain Maturation in Adolescence. *PLoS ONE* **9**, e83929 (2014).
137. M. H. Fung *et al.*, Pubertal Testosterone Tracks the Developmental Trajectory of Neural Oscillatory Activity Serving Visuospatial Processing. *Cerebral Cortex* **30**, 5960-5971 (2020).
138. A. D. Killanin *et al.*, Testosterone levels mediate the dynamics of motor oscillatory coding and behavior in developing youth. *Dev Cogn Neurosci* **61**, 101257 (2023).
139. M. H. Fung *et al.*, The development of sensorimotor cortical oscillations is mediated by pubertal testosterone. *Neuroimage* **264**, 119745 (2022).

140. G. Picci *et al.*, Developmental changes in endogenous testosterone have sexually-dimorphic effects on spontaneous cortical dynamics. *Human Brain Mapping* **44**, 6043-6054 (2023).
141. S. J. Kiebel, A. P. Kherif, C. Holmes, in *Statistical Parametric Mapping,* K. Friston, J. Ashburner, S. Kiebel, T. Nichols, W. Penny, Eds. (Academic Press, London, 2007), pp. 101-125.
142. J. L. Reed, N. M. Gallagher, M. Sullivan, J. H. Callicott, A. E. Green, Sex differences in verbal working memory performance emerge at very high loads of common neuroimaging tasks. *Brain and Cognition* **113**, 56-64 (2017).
143. D. Voyer, J. Saint Aubin, K. Altman, G. Gallant, Sex differences in verbal working memory: A systematic review and meta-analysis. *Psychol Bull* **147**, 352-398 (2021).
144. E. Barel, O. Tzischinsky, Age and Sex Differences in Verbal and Visuospatial Abilities. *Adv Cogn Psychol* **2**, 51-61 (2018).
145. J. M. Andreano, L. Cahill, Sex influences on the neurobiology of learning and memory. *Learning & Memory* **16**, 248-266 (2009).
146. E. Tzvi, L. Gajiyeva, L. Bindel, G. Hartwigsen, J. Classen, Coherent theta oscillations in the cerebellum and supplementary motor area mediate visuomotor adaptation. *Neuroimage* **251**, 118985 (2022).
147. S. P. Tomlinson, N. J. Davis, H. M. Morgan, R. M. Bracewell, Cerebellar contributions to spatial memory. *Neurosci Lett* **578**, 182-186 (2014).
148. E. Aminoff, N. Gronau, M. Bar, The parahippocampal cortex mediates spatial and nonspatial associations. *Cereb Cortex* **17**, 1493-1503 (2007).
149. R. A. Diana, Parahippocampal Cortex Processes the Nonspatial Context of an Event. *Cereb Cortex* **27**, 1808-1816 (2017).
150. M. Li, S. Lu, N. Zhong, The Parahippocampal Cortex Mediates Contextual Associative Memory: Evidence from an fMRI Study. *BioMed Research International* **2016**, 1-11 (2016).
151. D. Luck *et al.*, The right parahippocampal gyrus contributes to the formation and maintenance of bound information in working memory. *Brain Cogn* **72**, 255-263 (2010).
152. K. Schon, R. E. Newmark, R. S. Ross, C. E. Stern, A Working Memory Buffer in Parahippocampal Regions: Evidence from a Load Effect during the Delay Period. *Cereb Cortex* **26**, 1965-1974 (2016).
153. S. J. Short *et al.*, Correspondence between hair cortisol concentrations and 30-day integrated daily salivary and weekly urinary cortisol measures. *Psychoneuroendocrinology* **71**, 12-18 (2016).
154. T. W. Cheng *et al.*, A Researcher's Guide to the Measurement and Modeling of Puberty in the ABCD Study® at Baseline. *Frontiers in Endocrinology* **12**, (2021).